ATTITUDE DETERMINATION AND CONTROL OF NANO-SATELLITES

BY

JOHN GREGORY WARNER

THESIS

Submitted in partial fulfillment of the requirements
for the degree of Master of Science in Aerospace Engineering
in the Graduate College of the
University of Illinois at Urbana-Champaign, 2009

Urbana, Illinois

Adviser:

Professor Victoria Coverstone

ABSTRACT

The University of Illinois's IlliniSat2 satellite bus is unique in that it is among only a few nano-satellites that implements three-axis, onboard attitude determination and control. Though this is an ambitious goal, it will allow for a wide range of scientific missions to be accomplished on this bus. To complete the system, an accurate attitude determination system needs to be developed. Several methods for determining the attitude state as well as mitigating system noise are explored. In particular, an extended Kalman filter is developed to obtain accurate angular rate information from noisy rate measurements. These rate measurements may be provided by either rate gyros or by successive vector measurements. A linear Kalman filter is developed to obtain an accurate attitude estimate. The attitude may be measured with two vector measurements via the TRIAD algorithm, while sensor noise may be rejected via the filter. Using these techniques the requirements for an effective attitude determination and control system are met.

To all my family, especially my mom, dad, and brother, and friends who have tirelessly supported me.

ACKNOWLEDGMENTS

There are many people to thank who have made this research possible. First and foremost, many thanks to my advisor Professor Victoria Coverstone. Her guidance has been pivotal and always encouraging. A great deal of thanks is needed for all those involved with the IlliniSat project, Andy Pukniel in particular as well as Ryne Beeson and Joe Majcan. My best wishes go out to all those who will follow.

TABLE OF CONTENTS

LIST OF TABLES vii

LIST OF FIGURES viii

CHAPTER 1 INTRODUCTION 1

CHAPTER 2 CUBESAT OVERVIEW 2
2.1 CubeSat History 2
2.2 IlliniSat 2
2.3 Thesis Contributions 3

CHAPTER 3 ATTITUDE THEORY BACKGROUND 4
3.1 Reference Frames 4
3.1.1 Earth-Centered Inertial Reference Frame 4
3.1.2 Orbit Reference Frame 4
3.1.3 Satellite Fixed Body Reference Frame 5
3.2 Attitude Representations 6
3.2.1 Rotation Matrices 6
3.2.2 Euler Angles 7
3.2.3 Quaternions 9
3.2.4 Translation of Representations 10
3.3 Angular Velocity And Momentum 11
3.4 Rotational Dynamics And Kinematics 12

CHAPTER 4 ATTITUDE DETERMINATION THEORY 14
4.1 Three-Axis Determination 14
4.1.1 TRIAD Algorithm 15
4.2 Angular Rate Determination 16
4.3 Noise Mitigation Techniques 18
4.3.1 Moving Average 18
4.3.2 Kalman Filter Theory 18
4.3.3 Extended Kalman Filter Theory 21

CHAPTER 5 ILLINISAT ADACS ARCHITECTURE 23
5.1 Design Requirements 23
5.2 Attitude Determination Design Concept 25
5.3 Attitude Determination System Overview 25
5.4 Attitude Determination System Hardware Details 26
5.4.1 Angular Rate Extended Kalman Filter Derivation 28
5.4.2 Quaternion Kalman Filter Derivation 30
5.4.3 Attitude Control Summary 30

CHAPTER 6 SIMULATION RESULTS 33
6.1 System Simulator Description 33
6.2 Angular Rate Determination 35
6.2.1 Rate Gyro Simulation 35
6.2.2 Angular Rate Determination From Vector Measurements 38
6.3 Attitude Determination 40

CHAPTER 7 RECOMMENDATIONS AND FUTURE WORK 47
7.1 Recommendations 47
7.2 Future Work 47

REFERENCES 49

LIST OF TABLES

5.1 Attitude Control Requirements 23
5.2 Attitude Determination Requirements 24
5.3 ADACS Budget 24
5.4 Invensense Rate Gyro Characteristics 27
5.5 Rate Gyro Sensitivity Considerations 27
5.6 Honeywell Magnetometer Characteristics 28

6.1 Sensor Noise 34
6.2 Angular Rate Initial Conditions 35
6.3 EKF Simulation Error Standard Deviation Summary 36
6.4 Attitude Kalman Filter Simulation Error Deviation Summary 41

LIST OF FIGURES

3.1 Earth Centered Inertial Frame 5
3.2 Orbital Reference Frame 6
3.3 Satellite Body Frame 7

4.1 Successive Vector Measurements in Satellite Body Frame 17

5.1 Attitude Determination Concept 27

6.1 ADACS Simulator Concept 33
6.2 Tumbling Angular Rate Simulation With Rate Gyros Given Nominal Noise and High Rates . 36
6.3 Tracking Angular Rate Simulation With Rate Gyros Given Nominal Noise and Low Rates . . 37
6.4 Angular Rate Estimate From Vector Information With Diagonal Moment of Inertia 38
6.5 Angular Rate Estimate From Vector Information With Actual Moment of Inertia 39
6.6 RMS Error For Measured and Filtered Angular Rate Output Using Sun Sensor Vector Measurements With Nominal Noise Values 40
6.7 Measured and Filtered Attitude Given Nominal Noise and Tumbling 42
6.8 Pointing Knowledge Angular Error For One Orbit Given Nominal Noise and Tumbling 43
6.9 Refined Pointing Knowledge Angular Error For One Orbit Given Nominal Noise and Tumbling 44
6.10 Typical Attitude Filter Performance Given Nominal Noise and Tracking Angular Rates . . . 45
6.11 Refined Typical Attitude Filter Angular Error Given Nominal Noise and Tracking Angular Rates 46

CHAPTER 1

INTRODUCTION

Satellites have always been at the forefront of technological achievement. From the launch of Sputnik in 1957 to the most recent communications satellites, these devices have worked to extend what is possible. This realm, however, has up until recently been accessible only to those with the means to fund such endeavors. As technology continues to grow, a new domain in space systems has developed. Now, electronic components have reached a state where abundant functionality is available in a small package. Satellites are now able to be constructed on a small scale to complete meaningful tasks for much lower sums of money.

These nano-satellites are on the order of tens of kilograms and often hold an advantage over large scale satellites. Nano-satellites have the advantage of requiring much lower launch costs which enables designers to rethink the standard approach to risk management. This allows tasks which would be considered high risk for larger satellites to be completed, often gaining larger scientific rewards.

As nano-satellites are relatively inexpensive space systems, many non-traditional organizations, such as universities, have begun to develop satellites for scientific purposes. One of the more complex systems that few have implemented on a nano-satellite is attitude determination and control. There are a range of missions that would benefit from a capable attitude control system, such as remote sensing missions.

As the University of Illinois is a leader in technological research, it has begun developing the IlliniSat satellite bus to push the boundaries of functionality for nano-satellites. An important aspect of this is a three-axis attitude determination and control system.

This system has been under development for the past several years. While much work has been done to complete the attitude control system, this thesis develops the methodology to accurately determine attitude. First, a brief history of the IlliniSat program is given to establish the context of the work being done. The necessary background theory is then discussed so that the methods commonly used for attitude determination may be presented. The algorithms specifically used for the IlliniSat program are then developed. These include a series of Kalman filters which are used to accurately estimate the attitude. From here, the system is tested under a variety of conditions to show its ability. Finally, ultimate system recommendations are made and future work is summarized. With the completion of the attitude determination system, the IlliniSat bus has a functional system that allows a range of missions to be accomplished.

CHAPTER 2

CUBESAT OVERVIEW

2.1 CubeSat History

The CubeSat program began as a collaboration between professors at California Polytechnic State University and Stanford University in 1999. The goal of this partnership was to develop standards for the design and launch of nano-satellites. This was primarily accomplished by creating a standard launch deployment mechanism and standardizing the size of the nano-satellites contained within. By streamlining the launch process, the ability to access space has been increased.

All satellites that are launched from this standard deployer must prescribe to the CubeSat specification [1]. This document specifies the size of one unit as a 10 cm cube having a mass of up to 1.33 kg. Up to three units may be launched from a single deployer. Over 100 universities, schools and companies have developed a CubeSat with dozens of successful launches.

2.2 IlliniSat

The IlliniSat program began at the University of Illinois in 2001. Taught as a class, over 150 students have participated in the program. The first IlliniSat mission was known as Illinois Observing Nano-Satellite One (ION1). This two unit satellite's primary payload was a series of photometers used to remotely measure Oxygen chemistry in the upper atmosphere. The satellite was set to launch in July 2006; however, soon after lift off, the Dnepr launch vehicle commanded to abort the flight due to a malfunction in the first stage propulsion unit. All of the 18 satellites on-board, including ION1, were destroyed in the resulting crash.

Despite the loss of ION1, the IlliniSat program continued and began to develop IlliniSat2. The goal of IlliniSat2 is to create a generic satellite bus that will enable a range of scientific missions to occur. By confining the satellite to less than one cube unit, the remaining one or two units of space may be used for a range of payloads. This will allow the IlliniSat2 bus to be used with multiple missions.

2.3 Thesis Contributions

As the goal of IlliniSat2 is to create a bus that may be used for a range of scientific missions, a significant amount of work has been done on developing the Attitude Determination and Control System (ADACS). References [2] and [3] have documented what has been accomplished on the system so far. In particular, Reference [2] has developed a three axis attitude control system. This system was developed with the assumption that both the attitude and angular rates are accurately known at any time. There has been some work to develop a method of attitude determination, but it has previously had only limited success [3].

This thesis completes the ADACS by developing an attitude determination scheme. In conjunction with previous work, three-axis attitude determination and control may be implemented on IlliniSat2.

CHAPTER 3

ATTITUDE THEORY BACKGROUND

A spacecraft's attitude is defined as orientation of its body axes with respect to a given reference frame. There are a multitude of ways to describe three dimensional space, as well as orientation within that space. There are several reference frames and attitude representations that are used throughout the calculations below. These conventions are presented herein. Furthermore, the equations of motion that are pertinent to attitude are also discussed.

3.1 Reference Frames

An n-dimensional vector space may be fully described by a set n orthogonal basis vectors. A reference frame, or coordinate system, may then use these basis vectors to describe any vector in the space by its coordinates. There are several useful reference frames when considering a satellite in Earth's orbit.

3.1.1 Earth-Centered Inertial Reference Frame

The Earth-Centered Inertial (ECI) reference frame, is an inertial coordinate system with the origin at the center of the Earth. This coordinate frame will be denoted by I in the following formulations. The first of the coordinate axes, X_1^I , extends from the center of the Earth outwards in the direction of the First Point of Aries. This direction is typically measured on the vernal equinox of a specific day. Though this point is sufficiently far away so that it creates an inertial reference, it does precess. So, a specific date is needed to fully define this vector direction. As per previous calculations for IlliniSat, the J2000 reference frame will be used, which gives the epoch time at January 1st, 2000, 12:00:00.

The third reference vector, X_3^I , is defined from the center of the Earth extending through the North Pole. The remaining reference vector, X_2^I, is then defined by the typical vector cross product between X_1^I and X_3^I. Figure 3.1 contains a depiction of this reference frame.

3.1.2 Orbit Reference Frame

The Orbit Reference Frame (ORF) is not specifically used in calculations herein, but is included as a matter of completion and to aid understanding of previous work done on the IlliniSat attitude control system. This

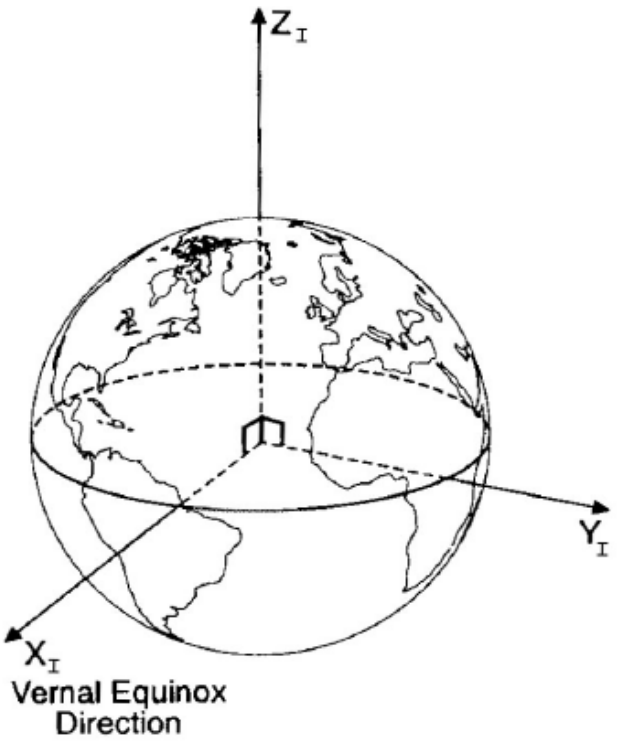

Figure 3.1: Earth Centered Inertial Frame
[4]

reference frame is centered on the satellite's moving center of mass and is denoted by R. Here, the X_3^R vector points from the origin to the center of the Earth, the X_1^R vector points from the origin in the direction of the velocity vector, and again, X_2^R is given by the vector cross product of the other two reference vectors. Figure 3.2 shows this reference frame.

3.1.3 Satellite Fixed Body Reference Frame

The Satellite Fixed Body (SFB) reference frame is the other most commonly used reference frame here; it is denoted by B in the following derivations. Again, the origin is fixed on the satellite's center of mass. Here, however, the reference vectors are always aligned with the geometry of the satellite. That is, the reference vectors rotate as the satellite rotates. The convention that will be used has X_3^B point along the long axis of the satellite. The X_1^B is pointing in the assembly model "positive X" direction. Again, the X_2^B reference vector is given as the cross product of the two. Figure 3.3 shows how these reference vectors are aligned on the satellite geometry.

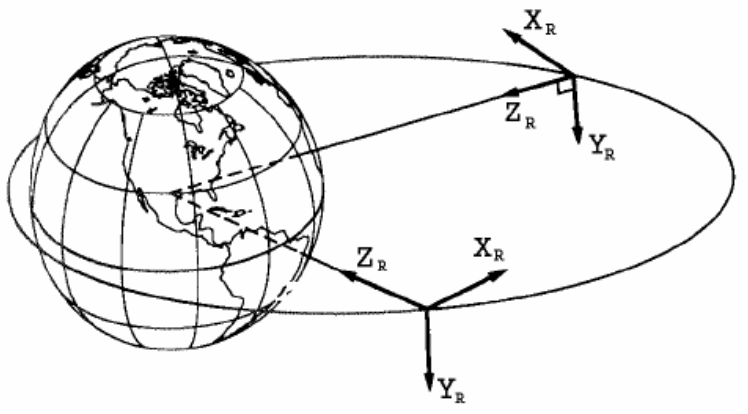

Figure 3.2: Orbital Reference Frame

3.2 Attitude Representations

Attitude is the description of one reference frame with respect to another reference frame. As one might imagine, there are many different methods for describing this mathematically. The several methods used for the subsequent calculations are described below. Each of these methods have their own advantages and disadvantages. Often, it is necessary to convert between the various representations to make use of these aspects.

3.2.1 Rotation Matrices

The most direct approach to representing attitude is a vector rotation matrix, or Direction Cosine Matrix (DCM) as it is often called. This matrix arises out of the fact that any given vector in one space may be decomposed along the vector bases of another vector space. Thus, for a given vector component in an arbitrary vector space A , it may be decomposed into the vector bases of an arbitrary vector space B .

$$x_A = \alpha_x x_B + \alpha_y y_B + \alpha_z z_B = \begin{bmatrix} \alpha_x & \alpha_y & \alpha_z \end{bmatrix} \begin{bmatrix} x_B \\ y_B \\ z_B \end{bmatrix} \tag{3.1}$$

So then, repeating this process for the y and z components, a matrix may be constructed.

$$\begin{bmatrix} x_A \\ y_A \\ z_A \end{bmatrix} = \begin{bmatrix} \alpha_x & \alpha_y & \alpha_z \\ \beta_x & \beta_y & \beta_z \\ \gamma_x & \gamma_y & \gamma_z \end{bmatrix} \begin{bmatrix} x_B \\ y_B \\ z_B \end{bmatrix} = A^{A/B} \begin{bmatrix} x_B \\ y_B \\ z_B \end{bmatrix} \tag{3.2}$$

The matrix $A^{A/B}$ is the rotation matrix or DCM. The DCM is a linear operator that represents a vector rotation from one reference frame to another reference frame. Physically, each element of the matrix rep-

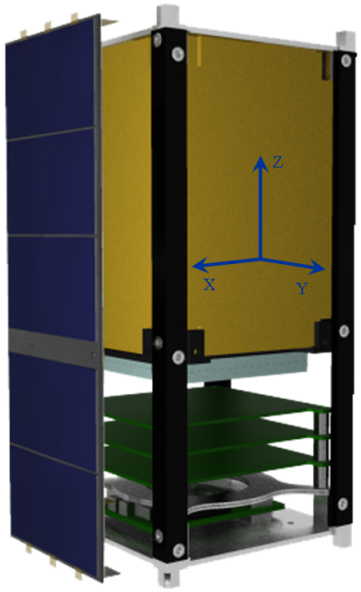

Figure 3.3: Satellite Body Frame
[4]

resents the cosine of the angle between the original vector base and the vector rotated into the new base vector.

The DCM has the advantage of having a clear physical significance and being an orthonormal matrix. Furthermore, subsequent rotations may be represented by multiplying a series of DCM together. The DCM, however, is not used frequently in calculations as it is mathematically cumbersome. There are only three independent quantities for rotation, but the DCM contains nine components. So, there are six redundant components, which makes computations involving the DCM unnecessarily intensive.

3.2.2 Euler Angles

In order to reduce the number of quantities used in describing the attitude, any given orientation may be represented as a series of three successive rotations by angles ψ, θ, and ϕ. In general, these angles are referred to as the roll, pitch and yaw angles, respectively. As an example of the Euler angle formulation, consider a rotation about the X_3 axis by ψ is performed, followed by a rotation of θ about the resulting X_2' axis, and finally a rotation by ϕ about the final X_1'' axis. There are, however, various conventions used as an attitude state may be described by three successive rotations about each axis in any order. The convention used by IlliniSat is the R_{321}, which is the one given above.

It is possible to write an expression relating the original reference frame to the rotated reference frame based only on the angles of rotation. Consider the first rotation about the X_3 axis.

$$\begin{bmatrix} X'_1 \\ X'_2 \\ X'_3 \end{bmatrix} = R_3(\psi) \begin{bmatrix} X_1 \\ X_2 \\ X_3 \end{bmatrix} = \begin{bmatrix} \cos(\psi) & \sin(\psi) & 0 \\ -\sin(\psi) & \cos(\psi) & 0 \\ 0 & 0 & 1 \end{bmatrix} \begin{bmatrix} X_1 \\ X_2 \\ X_3 \end{bmatrix} \tag{3.3}$$

Now, consider a second rotation about the new X'_2 axis by the angle θ, and finally a third rotation about the new X''_1 axis by the angle ϕ.

$$\begin{bmatrix} X''_1 \\ X''_2 \\ X''_3 \end{bmatrix} = R_2(\theta) \begin{bmatrix} X'_1 \\ X'_2 \\ X'_3 \end{bmatrix} = \begin{bmatrix} \cos(\theta) & 0 & -\sin(\theta) \\ 0 & 1 & 0 \\ \sin(\theta) & 0 & \cos(\theta) \end{bmatrix} \begin{bmatrix} X'_1 \\ X'_2 \\ X'_3 \end{bmatrix} \tag{3.4}$$

$$\begin{bmatrix} X'''_1 \\ X'''_2 \\ X'''_3 \end{bmatrix} = R_1(\phi) \begin{bmatrix} X''_1 \\ X''_2 \\ X''_3 \end{bmatrix} = \begin{bmatrix} 1 & 0 & 0 \\ 0 & \cos(\phi) & \sin(\phi) \\ 0 & -\sin(\phi) & \cos(\phi) \end{bmatrix} \begin{bmatrix} X''_1 \\ X''_2 \\ X''_3 \end{bmatrix} \tag{3.5}$$

A total rotation matrix may be then found substituting in for X' and X'', so that the final coordinates are expressed as a product of the three rotation matrices and the original coordinates.

$$\begin{bmatrix} X_1''' \\ X_2''' \\ X_3''' \end{bmatrix} = R_1(\phi) R_2(\theta) R_3(\psi) \begin{bmatrix} X_1 \\ X_2 \\ X_3 \end{bmatrix} \tag{3.6}$$

$$\begin{bmatrix} X_1''' \\ X_2''' \\ X_3''' \end{bmatrix} = R_{321} \begin{bmatrix} X_1 \\ X_2 \\ X_3 \end{bmatrix} \tag{3.7}$$

$$R_{321} = \begin{bmatrix} \cos(\psi)\cos(\theta) & \sin(\psi)\cos(\theta) & -\sin(\theta) \\ -\sin(\psi)\cos(\phi) + \cos(\psi)\sin(\theta)\cos(\phi) & \cos(\psi)\cos(\phi) + \sin(\psi)\sin(\theta)\sin(\phi) & \cos(\theta)\sin(\phi) \\ \sin(\psi)\sin(\phi) + \cos(\psi)\sin(\theta)\cos(\phi) & -\cos(\psi)\sin(\phi) + \sin(\psi)\sin(\theta)\cos(\phi) & \cos(\theta)\cos(\phi) \end{bmatrix}$$

Upon inspection of each rotation matrix, it is evident that the matrix is orthonormal. Since the product of an orthonormal matrix is itself orthonormal, the R_{321} matrix is orthonormal. Thus, the inverse rotation can be mapped by the transpose of this matrix.

This formulation has the advantage of having a clear physical meaning. Each angle is clearly a rotation about the satellite body fixed axes. However, computationally, trigonometric functions are more expensive and have the added disadvantage that they are not globally continuous. These characteristics make Euler angles generally not suitable for use in flight.

3.2.3 Quaternions

The last attitude representation to be discussed is the attitude Quaternion. A quaternion is a four element vector that can be used to represent attitude. The first three elements of this vector describe an axis of rotation, while the fourth element describes the angle of rotation about this axis. So, a transformation for reference frame A to B can be represented as the following equation.

$$\mathbf{q}^{A/B} = \begin{bmatrix} q_1^{A/B} \\ q_2^{A/B} \\ q_3^{A/B} \\ q_4^{A/B} \end{bmatrix} \tag{3.8}$$

Furthermore, a quaternion is a unit normal vector. So, the following is satisfied.

$$\|\mathbf{q}\| = 1 \tag{3.9}$$

Quaternions are non-commutative, so mathematical operators do not behave in the same manner as for standard vectors. Multiplication of quaternions is defined by the following method. Consider the three following quaternions.

$$\mathbf{q}^{A/B} = \begin{bmatrix} q_1 \\ q_2 \\ q_3 \\ q_4 \end{bmatrix} \qquad \mathbf{q}^{B/C} = \begin{bmatrix} q_1' \\ q_2' \\ q_3' \\ q_4' \end{bmatrix} \qquad \mathbf{q}^{A/C} = \begin{bmatrix} q_1'' \\ q_2'' \\ q_3'' \\ q_4'' \end{bmatrix} \tag{3.10}$$

So then, multiplying the quaternions together yields the following.

$$\mathbf{q}^{A/C} = \mathbf{q}^{A/B} \otimes \mathbf{q}^{B/C}$$

$$\mathbf{q}^{A/C} = \begin{bmatrix} q_4' & q_3' & -q_2' & q_1' \\ -q_3' & q_4' & q_1' & q_2' \\ q_2' & -q_1' & q_4' & q_3' \\ -q_1' & -q_2' & -q_3' & -q_4' \end{bmatrix} \begin{bmatrix} q_1 \\ q_2 \\ q_3 \\ q_4 \end{bmatrix} = \begin{bmatrix} q_4 & -q_3 & q_2 & q_1 \\ q_3 & q_4 & -q_1 & q_2 \\ -q_2 & q_1 & q_4 & q_3 \\ -q_1 & -q_2 & -q_3 & q_4 \end{bmatrix} \begin{bmatrix} q_1' \\ q_2' \\ q_3' \\ q_4' \end{bmatrix} \tag{3.11}$$

It should also be noted that a quaternion is equal to its negative. That is, for any given axis and angle of rotation specified by a quaternion, and identical attitude can be described by the opposite axis and angle of rotation. The following equation demonstrates this.

$$\mathbf{q} = \begin{bmatrix} q_1 \\ q_2 \\ q_3 \\ q_4 \end{bmatrix} = \begin{bmatrix} -q_1 \\ -q_2 \\ -q_3 \\ -q_4 \end{bmatrix} = -\mathbf{q} \tag{3.12}$$

Quaternions have the advantage of only having four terms. Thus, quaternion calculations are not as computationally intensive as with another attitude representation, say, the direction cosine matrix. Furthermore, quaternions are defined and globally continuous for any attitude, so they are beneficial for calculations. It is for these reasons that the attitude of IlliniSat will generally be represented as a quaternion. The only disadvantage to this system is that there is no intuitive physical meaning behind the parameters; however, a quaternion can easily be translated into any other attitude representation.

3.2.4 Translation of Representations

Each of aforementioned attitude representations may be freely translated from one form to another. First, the attitude matrix that results from the Euler Angle formulation may be easily converted to recover the roll, pitch and yaw angles. Upon inspection of this matrix, the following formulas become clear.

Given a_{ij} represent the component of the DCM.

$$\begin{aligned} \phi &= arctan\left(\frac{a_{23}}{a_{33}}\right) \\ \theta &= -arcsin\left(a_{13}\right) \\ \psi &= arctan\left(\frac{a_{12}}{a_{11}}\right) \end{aligned} \tag{3.13}$$

Next, the conversions can be made between the DCM and quaternions in both directions. For a given $\mathbf{q}$, the attitude matrix can be expressed as the following.

$$A = \begin{bmatrix} q_1^2 - q_2^2 + q_3^2 + q_4^2 & 2(q_1q_2 + q_3q_4) & 2(q_1q_3 - q_2q_4) \\ 2(q_1q_2 - q_3q_4) & -q_1^2 + q_2^2 - q_3^2 + q_4^2 & 2(q_1q_4 + q_2q_3) \\ 2(q_1q_3 + q_2q_4) & 2(q_2q_3 - q_1q_4) & -q_1^2 - q_2^2 + q_3^2 + q_4^2 \end{bmatrix} \tag{3.14}$$

A given quaternion can also be expressed in terms of components of the DCM. The formula, however, normalizes each component of $\mathbf{q}$ by one specific component. So, there are four different formulas to determine this to avoid the singularity if one component approaches zero. Only two algorithms are given below; one normalizing by q_4, the other normalizing by q_1. This is because generally q_1 and q_4 do not approach zero at the same time.

$$
\begin{aligned}
q_1 &= \frac{1}{4q_4}\left(a_{23} - a_{32}\right) \\
q_2 &= \frac{1}{4q_4}\left(a_{31} - a_{13}\right) \\
q_3 &= \frac{1}{4q_4}\left(a_{12} - a_{21}\right) \\
q_4 &= \pm\frac{1}{2}(1 + a_{11} + a_{22} + a_{33})^{1/2}
\end{aligned}
\tag{3.15}
$$

It should be noted that the sign ambiguity in q_4 may be evaluated in either manner with no consequences on the final result as $\mathbf{q} = -\mathbf{q}$ for any $\mathbf{q}$. The second algorithm based on normalizing by q_1 is given below.

$$
\begin{aligned}
q_1 &= \pm\frac{1}{2}(1 + a_{11} - a_{22} - a_{33})^{1/2} \\
q_2 &= \frac{1}{4q_1}\left(a_{12} - a_{21}\right) \\
q_3 &= \frac{1}{4q_1}\left(a_{13} - a_{31}\right) \\
q_4 &= \frac{1}{4q_1}\left(a_{23} - a_{32}\right)
\end{aligned}
\tag{3.16}
$$

Finally, an attitude expressed in $\mathbf{q}$ may be expressed in roll, pitch and yaw angles by intermediately converting to the DCM matrix.

3.3 Angular Velocity And Momentum

The rate of change of the attitude can be thought of as the angular velocity. Specifically, the rate of rotation of one reference frame with respect to another frame is the angular velocity. The rate of change of the reference frame A with respect to B is donated as $\omega^{A/B}$. This quantity has the following property

$$
\omega^{A/B} = -\omega^{B/A} \tag{3.17}
$$

In addition, angular velocity is commutable, so that the following equation is true.

$$
\omega^{A/C} = \omega^{A/B} + \omega^{B/C} \tag{3.18}
$$

Derivatives of a vector in one reference frame may be expressed in another reference frame even if the frames are moving relative to each other. For example, consider a vector $\mathbf{R}$ in the A frame which rotates with respect to the B frame with angular velocity given by $\omega^{A/B}$.

$$
\begin{aligned}
\dot{\mathbf{R}}^B &= \dot{\mathbf{R}}^A + \omega^{A/B} \times \mathbf{R}^B \\
\dot{\mathbf{R}}^A &= \dot{\mathbf{R}}^B + \omega^{B/A} \times \mathbf{R}^A
\end{aligned}
\tag{3.19}
$$

Further, as linear momentum may be expressed for linear velocity, angular momentum may be expressed for angular velocity. Angular momentum, $\mathbf{h}$, is defined as the following.

$$\mathbf{h} = \tilde{I}\,\omega^{B/I} \tag{3.20}$$

Here, $\tilde{I}$ is the moment of inertia matrix and $\omega^{B/I}$ is the angular velocity. Note that the angular momentum may be expressed in terms of any reference frame.

3.4 Rotational Dynamics And Kinematics

Newton's laws of motion relate the time rate of change of momentum to the force on an object. This relation may be applied to the angular momentum, so that the following equation is true.

$$\dot{\mathbf{h}}_I = \tau \tag{3.21}$$

Here, $\dot{\mathbf{h}}_I$ refers to the time rate of change of the angular momentum with respect to the inertial reference frame and τ is the total torque on the system. Now using Equation 3.19, the angular velocity in body frame may be derived.

$$\dot{\mathbf{h}}_B = \tau - \omega^{B/I} \times \mathbf{h} \tag{3.22}$$

It can be seen that the following is true given the definition of the angular momentum.

$$\dot{\mathbf{h}}_B = \frac{d}{dt}\left(\tilde{I}\,\omega^{B/I}\right) = \tilde{I}\,\dot{\omega}^{B/I} \tag{3.23}$$

Using the above equations, the following expression for the time rate of change of the angular velocity derived.

$$\dot{\omega}^{B/I} = \tilde{I}^{-1}\left(\tau - \omega^{B/I} \times (\tilde{I}\,\omega^{B/I})\right) \tag{3.24}$$

Note that by definition the moment of inertial matrix is positive definite so that an inverse always exists.

Last, the equation for the time rate of change of the quaternion is needed to propagate the system dynamics. See Reference [4] for a more complete derivation of the below equation. The time rate of change of the quaternion is given by the following.

$$\dot{\mathbf{q}}^{B/I} = \frac{1}{2}\begin{bmatrix} 0 & \omega_3 & -\omega_2 & \omega_1 \\ -\omega_3 & 0 & \omega_1 & \omega_2 \\ \omega_2 & -\omega_1 & 0 & \omega_3 \\ -\omega_1 & -\omega_2 & -\omega_3 & 0 \end{bmatrix}\begin{bmatrix} q_1 \\ q_2 \\ q_3 \\ q_4 \end{bmatrix} \tag{3.25}$$

Note, the time rate of change of the quaternion is linear with respect to the angular rates. So similarly, the time rate of change of the quaternion can be expressed as a linear combination of the angular rates in the following manner.

$$\dot{\mathbf{q}}^{B/I} = \frac{1}{2}\begin{bmatrix} q_4 & -q_3 & q_2 & q_1 \\ q_3 & q_4 & -q_1 & q_2 \\ -q_2 & q_1 & q_4 & q_3 \\ -q_1 & -q_2 & -q_3 & q_4 \end{bmatrix}\begin{bmatrix} \omega_1 \\ \omega_2 \\ \omega_3 \\ 0 \end{bmatrix} \tag{3.26}$$

In addition, it useful to express Equation 3.25 in terms of a state transition matrix, so that dynamics may be easily propagated forward in time. The state transition matrix can be given by the following equation.

$$\Phi = \mathcal{L}^{-1}\left(s\,I - A\right)^{-1} \tag{3.27}$$

Here, s is the complex parameter used in the Laplace transform, I is the identity matrix, and A is the constant state dynamics matrix. Applying this process, the attitude dynamics may be expressed in the following manner. For linear dynamics, as expressed below.

$$\dot{\mathbf{x}} = A\,\mathbf{x} \tag{3.28}$$

Then the state transition matrix can be calculated as follows.

$$\mathbf{q}_k = \Phi\,\mathbf{q}_{k-1} \tag{3.29}$$

The state transition matrix Φ is given in terms of the angular rate vector ω by the following.

$$\Phi = \begin{bmatrix} cos(\frac{1}{2}\,\Omega\,dt) & \frac{\omega_3}{\Omega}\,sin(\frac{1}{2}\,\Omega\,dt) & -\frac{\omega_2}{\Omega}\,sin(\frac{1}{2}\,\Omega\,dt) & \frac{\omega_1}{\Omega}\,sin(\frac{1}{2}\,\Omega\,dt) \\ -\frac{\omega_3}{\Omega}\,sin(\frac{1}{2}\,\Omega\,dt) & cos(\frac{1}{2}\,\Omega\,dt) & \frac{\omega_1}{\Omega}\,sin(\frac{1}{2}\,\Omega\,dt) & \frac{\omega_2}{\Omega}\,sin(\frac{1}{2}\,\Omega\,dt) \\ \frac{\omega_2}{\Omega}\,sin(\frac{1}{2}\,\Omega\,dt) & -\frac{\omega_1}{\Omega}\,sin(\frac{1}{2}\,\Omega\,dt) & cos(\frac{1}{2}\,\Omega\,dt) & \frac{\omega_3}{\Omega}\,sin(\frac{1}{2}\,\Omega\,dt) \\ -\frac{\omega_1}{\Omega}\,sin(\frac{1}{2}\,\Omega\,dt) & -\frac{\omega_2}{\Omega}\,sin(\frac{1}{2}\,\Omega\,dt) & -\frac{\omega_3}{\Omega}\,sin(\frac{1}{2}\,\Omega\,dt) & cos(\frac{1}{2}\,\Omega\,dt) \end{bmatrix} \tag{3.30}$$

Here, $\Omega = ||\omega||$.

CHAPTER 4

ATTITUDE DETERMINATION THEORY

A spacecraft's attitude is defined as the orientation of the body-fixed reference frame with respect to another reference frame. The goal of the IlliniSat bus is to have a system that can determine and control the spacecraft's attitude on all three axes, on-board in real time. This goal is necessary as the bus is designed to enable a wide range of scientific missions that require precise pointing knowledge and control.

There are several methods for determining attitude and mitigating the effects of sensor noise. These methods are discussed in detail below.

4.1 Three-Axis Determination

In order to fully determine attitude along all three axes, two measurements in the body frame and two reference vectors in the reference frame are needed [4].

This at first glance, may sound counterintuitive. However, one may realize that given only one measurement and one reference vector there are only two independent pieces of information. This is due to the fact that both vectors are constrained to have equivalent magnitude, thus making one of the components of the attitude dependent upon the other two. As an additional example, one may view attitude as the three consecutive rotations that align one vector basis with a second vector basis. Consider one vector aligned with the X axis of the first vector basis and the second vector aligned with the X' axis on the second basis. After two angular rotations, both vectors are aligned and remained aligned for any third rotation; that is, any final rotation about the X axis will keep the vectors aligned, thus making it undetermined.

Without this knowledge, it is possible to infer the attitude using a Kalman filter. One method for attitude determination using only a magnetometer is outlined in an article by Psiaki [5]. This option has been pursued at various time in the IlliniSat program, yet has yielded no success [3]. The main difficulty is that this method requires the three components of attitude and three angular rates to be inferred from the two pieces of information provided by the magnetometer. The dynamics may not be observable over reasonable time scales.

For these reasons, it has been decided that the system design should include a sufficient amount of sensors so that the dynamics are observable at any time. This then allows the system to always operate within an known margin of error and provides a more adaptable solution as the IlliniSat bus evolves to meet the

requirements of yet unknown missions.

4.1.1 TRIAD Algorithm

A common method to determine attitude from two measurements and two reference vectors is the TRIAD method [6]. Consider the measurement vectors $\mathbf{m_1}$ and $\mathbf{m_2}$ in the body frame, and the corresponding reference vectors $\mathbf{r_1}$ and $\mathbf{r_2}$ in the reference frame (the inertial frame will be used here for example). First three vectors are created in the following manner.

$$\begin{aligned} \mathbf{t_1} &= \frac{\mathbf{m_1}}{|\mathbf{m_1}|} \\ \mathbf{t_2} &= \frac{\mathbf{m_1} \times \mathbf{m_2}}{|\mathbf{m_1} \times \mathbf{m_2}|} \\ \mathbf{t_3} &= |\mathbf{t_1} \times \mathbf{t_2}| \end{aligned} \tag{4.1}$$

These three vectors can be used to create a vector basis in an intermediate reference frame. This can be use to create a direction cosine matrix (DCM) from the body frame to an intermediate frame (denoted by t) where the vector basis is represented by the three vectors above. So the following is true.

$$A^{B/t} = \begin{bmatrix} \mathbf{t_1} & \mathbf{t_2} & \mathbf{t_3} \end{bmatrix} \tag{4.2}$$

Similarly, three vectors can be created from the reference vectors.

$$\begin{aligned} \mathbf{s_1} &= \frac{\mathbf{r_1}}{|\mathbf{r_1}|} \\ \mathbf{s_2} &= \frac{\mathbf{r_1} \times \mathbf{r_2}}{|\mathbf{r_1} \times \mathbf{r_2}|} \\ \mathbf{s_3} &= |\mathbf{s_1} \times \mathbf{s_2}| \end{aligned} \tag{4.3}$$

These three vectors form a vector basis in the intermediate frame and may be used to create a DCM from the inertial frame to the intermediate frame.

$$A^{I/t} = \begin{bmatrix} \mathbf{s_1} & \mathbf{s_2} & \mathbf{s_3} \end{bmatrix} \tag{4.4}$$

So then, the DCM from the body frame to the inertial frame may be found using the properties of the DCM and orthonormal matrices.

$$\begin{aligned} A^{B/I} &= A^{B/t}\, A^{t/I} \\ &= A^{B/t}\, (A^{I/t})^{-1} \\ &= A^{B/t}\, (A^{I/t})^{T} \end{aligned} \tag{4.5}$$

Equivalently, the above may be written in the following manner.

$$A^{B/I} = \mathbf{t_1} \cdot \mathbf{s_1^T} + \mathbf{t_2} \cdot \mathbf{s_2^T} + \mathbf{t_3} \cdot \mathbf{s_3^T} \tag{4.6}$$

Thus, for any two measurement vectors and the two corresponding reference vectors, the attitude may be determined.

4.2 Angular Rate Determination

Knowledge of how fast the satellite is spinning while in orbit is important so that precise control can be applied. There are two methods that were explored to determine the angular rates.

First, rate gyros may be added to the sensor suite so that the angular rates may be directly measured. This option has the advantage that performance is guaranteed within a given margin and that the rates may be sampled at any time. However, this also presents the challenge of integrating additional hardware. Performance is largely hardware dependent.

Second, an algorithm was developed to determine the angular rates from a series of magnetic field readings. This technique makes use of the fact that the angular rate vector can be separated into one direction and the magnitude of the rates in the body frame. The direction of rotation will be noted $\hat{\omega}$, and the magnitude of rotation will be given by the scalar ω.

Now, a geometrical approach is taken to determine the direction of rotation. First consider a vector $\mathbf{P}$ fixed in inertial space and a rotating satellite with body frame B. Now consider three successive measurements: $\mathbf{P_1}$, $\mathbf{P_2}$ and $\mathbf{P_3}$, where $\mathbf{P_3}$ is the most recent vector. Given these three points, a plane may be formed. The vector normal to this plane is the direction of rotation. Figure 4.1 shows a depiction of this. Notice the path the measured Sun position vector tracs on the attitude sphere is a circle and that angular rate vector is perpendicular to that circle.

So, any three succesive measurements will define this plane. The normal vector of this plane will give the

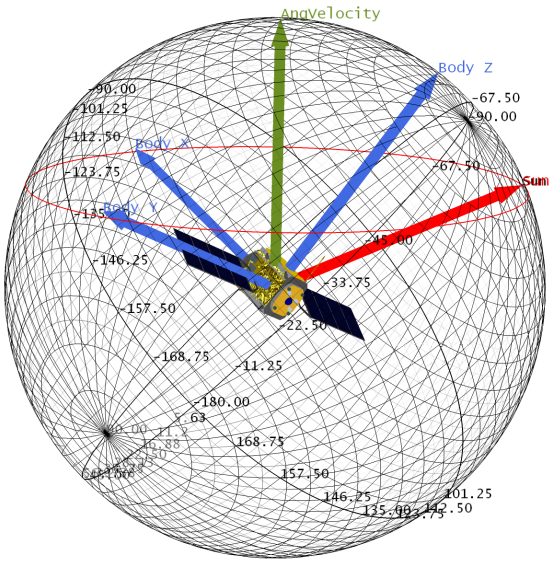

Figure 4.1: Successive Vector Measurements in Satellite Body Frame

direction of rotation. The following formula gives the vector normal to a three point plane.

$$\begin{aligned} \mathbf{P_a} &= \mathbf{P_1} - \mathbf{P_3} \\ \mathbf{P_b} &= \mathbf{P_2} - \mathbf{P_3} \end{aligned} \tag{4.7}$$

Given the above constructed vectors, the normal vector is as follows.

$$\hat{\omega} = \frac{\mathbf{P_a} \times \mathbf{P_b}}{|\mathbf{P_a} \times \mathbf{P_b}|} \tag{4.8}$$

The magnitude of the angular rates can be found in one of two manners. First, the fast Fourier transform (FFT) of the magnetic field readings may be taken. This process transforms the measurements from the time domain to the frequency domain. The frequency at which the readings vary is the frequency of rotation. This technique has the advantage that it is generally easy to separate random noise, which is evenly distributed across the noise spectrum, from the frequency of rotation.

A second method may be accomplished by calculating the angular displacement between the vectors $\mathbf{P_a}$ and $\mathbf{P_b}$. Given the sample rate it is possible to calculate the rate of change. However, the process is essentially a numerical derivative and thus will cause noise amplification.

4.3 Noise Mitigation Techniques

In any physical system, sensor noise is always present. This noise has the negative effect of decreasing system accuracy. In order to reach the precision that is necessary, several techniques are investigated to mitigate this noise. The techniques investigated are both dynamics-based and non-dynamics-based.

4.3.1 Moving Average

One technique that is easy to implement to mitigate noise is a moving average filter. An example of this would be the simple moving average, which averages only a set number of the most recent samples; this number of samples will be referred to as the window size. Consider a measurement $\mathbf{m}$ and a window size n, the averaged output is given below.

$$\mathbf{m_{avg}} = \sum_{i=1}^{n} \frac{\mathbf{m}}{n} \tag{4.9}$$

This is called a simple moving average since each term carries an identical weight. Other moving averages may be taken by providing different weights for each term. This is done because the output of this filter tends to lag the signal continuously. This may be partially mitigated by placing a higer weight on the more recent terms. One filter that does this is the exponential moving average. The formula for this is given below.

$$\begin{aligned} \alpha &= \frac{2}{n+1} \\ \mathbf{m_{avg_i}} &= \alpha \cdot \left(\mathbf{m}_1 + (1-\alpha)\,\mathbf{m}_2 + (1-\alpha)^2\,\mathbf{m}_3 + \ldots + (1-\alpha)^{n-1}\,\mathbf{m}_n\right) \end{aligned} \tag{4.10}$$

This may be further defined recursively as given below.

$$\mathbf{m_{avg_i}} = \mathbf{m_{avg_{i-1}}} + \alpha \cdot \left(\mathbf{m_i} - \mathbf{m_{avg_{i-1}}}\right) \tag{4.11}$$

These techniques represent a basic method of mitigating system noise. Reference [7] contains the derivation and further information on these concepts.

4.3.2 Kalman Filter Theory

Another technique for mitigating system noise is a Kalman filter (KF). This filter makes use of the fact that dynamics of the quantities being filter are known and can be modeled prior to filtering. The Kalman filter is an optimal minimum variance linear state estimator. Essentially, the filter works in two steps: first, the state dynamics are propagated forward in time from the current estimate; second, that propagated state is optimally corrected by the measurement from the sensors. The original derivation may be found in Reference [8], while a concise summary may be found in Reference [9].

The Kalman filter makes use of the standard linear system dynamics.

$$\mathbf{x}_k = A\mathbf{x}_{k-1} + B\mathbf{u}_{k-1} + \mathbf{w}_{k-1} \tag{4.12}$$

Here, a state $\mathbf{x}$ at time k is a linear function of the previous state, $\mathbf{x}_{k-1}$, the control at the previous time, $\mathbf{u}_{k-1}$, and random white noise, $\mathbf{w}_{k-1}$. The matrix A relates the state at the previous time to the state at the current time. This matrix is sometimes known as the state transition matrix. Similarly, the matrix B relates the state at the current time to the control at the previous time. The state measurement, $\mathbf{z}$, is then given by the equation below.

$$\mathbf{z}_k = H\mathbf{x}_k + \mathbf{v}_k \tag{4.13}$$

Here, $\mathbf{v}$ is again a random white noise and the matrix H relates the measurement of the state to the state itself. The probability distribution is characterized by the expected value, denoted by the operator E, and the variance, denoted by σ. The above random noise variables have the following characteristics.

$$\begin{aligned} E(\mathbf{w}) &= 0 \\ \sigma(\mathbf{w}) &= Q \\ E(\mathbf{v}) &= 0 \\ \sigma(\mathbf{v}) &= R \end{aligned} \tag{4.14}$$

Here, the covariance of $\mathbf{w}$, represented by the matrix Q, is called the process noise covariance. This quantity encompasses noise due to unmodeled dynamics, such as disturbances. The covariance of $\mathbf{v}$, denoted by R, is called the measurement noise covariance. This quantity represents the noise that can be attributed to sensor noise.

Given the above equations, the system dynamics as well as the statistical distribution of sources of error are described. With this information, an estimation of the state can be made. The estimation of the state is denoted by $\hat{\mathbf{x}}$.

The Kalman filter makes two state estimates at any given time step. The first estimate is given by propagated dynamics, that is, before the measurement, and is denoted by $\hat{\mathbf{x}}^-$. The final estimate is made after the measurement and is represented by $\hat{\mathbf{x}}$. Given this, two equations for system error related to the true state, $\mathbf{x}$, can be written. The first equation represents the error before the measurement, while the second represents the error after the measurement.

$$\begin{aligned} \mathbf{e}_k^- &= \mathbf{x}_k - \hat{\mathbf{x}}^- \\ \mathbf{e}_k &= \mathbf{x}_k - \hat{\mathbf{x}} \end{aligned} \tag{4.15}$$

With this, the error covariance can be defined in the following manner.

$$P_k^- = E\left[e_k^-\, e_k^{-T}\right] \tag{4.16}$$

$$P_k = E\left[e_k\, e_k{}^T\right] \tag{4.17}$$

This matrix P can be thought of as the error variance of each component of the state with respect to the other components of the state and itself. The Kalman filter is then derived by finding how to optimally minimize the state error covariance given the system dynamics and a series of state measurements. As the full derivation is somewhat complex, just the results will be summarized here. The original derivation can be found in Reference [8].

The first step of a Kalman filter is to propagate the state forward in time given the dynamics that are modeled.

$$\hat{\mathbf{x}}_k^- = A\hat{\mathbf{x}}_{k-1} + B\mathbf{u}_{k-1} \tag{4.18}$$

$$P_k^- = A\, P_{k-1}\, A^T + Q \tag{4.19}$$

In the above equation, notice that both the state and error covariance matrix are both projected forward in time. Next, information from the state measurement must be used to improve the estimate. This is done by calculating the optimal gain for the measurement given the statistical distribution of system and process noise. The final estimate is then calculated and the error covariance is updated.

$$\hat{\mathbf{x}}_k = \hat{\mathbf{x}}_k^- + K_k\, \left(\mathbf{z}_k - H\, \hat{\mathbf{x}}_k^-\right) \tag{4.20}$$

$$P_k = (I - K_k\, H)\; P_k^- \tag{4.21}$$

The optimal gain K is given by the following equation.

$$K_k = P_k^- H^T \left(H P_k^- H^T + R\right)^{-1} \tag{4.22}$$

It can be seen from the above equations that the final state estimate is the propagated state that has been corrected by what is known as the residual, given by $\mathbf{z}_k - H\, \hat{\mathbf{x}}_k^-$ multiplied by the Kalman gain, which is give by the matrix K. Thus, the final state is given by the propagated state which is then optimally adjusted by the difference between the measurement and the propagated stated. This process provides the minimum variance linear estimate of the state.

4.3.3 Extended Kalman Filter Theory

The Kalman filter does not provide an optimal estimate for any system that is not described by linear dynamics. However, the Kalman filter equations may be applied to a non-linear system by linearizing the dynamics. This filter is known as an extended Kalman filter (EKF). This system is not considered optimal, but generally achieves high performance for minimal complexity. Reference [10] contains a more detailed development of this topic.

Consider system dynamics described by a general function.

$$\mathbf{x}_k = f\left(\mathbf{x}_{k-1}, u_{k-1}, w_{k-1}\right) \tag{4.23}$$

The measurement may also be given by a general function.

$$\mathbf{z}_k = h\left(\mathbf{x}_k, \mathbf{v}_k\right) \tag{4.24}$$

For simplicity, it will be assumed that the functions f and h are linear with respect to the process noise and measurement noise. The Jacobian matrices of the derivatives of f and h with respect to $\mathbf{x}$ are needed.

$$A_{[i,j]} = \frac{\partial f_i}{\partial x_j}\left(\hat{\mathbf{x}}_{k-1}, \mathbf{u}_{k-1}, 0\right) \tag{4.25}$$

$$H_{[i,j]} = \frac{\partial h_i}{\partial x_j}\left(\hat{\mathbf{x}}_{k-1}, 0\right) \tag{4.26}$$

The equations for the EKF are similar to that of the standard Kalman filter. First, the dynamics and the error covariance are propagated forward in time.

$$\hat{\mathbf{x}}_k^- = f\left(\hat{\mathbf{x}}_{k-1}, \mathbf{u}_{k-1}, 0\right) \tag{4.27}$$

$$P_k^- = A_k P_{k-1} A_k^T + Q_{k-1} \tag{4.28}$$

Next, the state estimate is updated by the measurement.

$$\hat{\mathbf{x}}_k = \hat{\mathbf{x}}_k^- + K_k\left(\mathbf{z}_k - h(\hat{\mathbf{x}}_k^-, 0)\right) \tag{4.29}$$

$$P_k = \left(I - K_k H_k\right) P_k^- \tag{4.30}$$

The Kalman gain is given by the following expression.

$$K_k = P_k^- H_k^T \left(H_k P_k^- H_k^T + R_k\right)^{-1} \tag{4.31}$$

Again, the EKF does not provide an optimal state estimate as it linearizes the system dynamics so that

they prescribe to the necessary form for a Kalman filter. An EKF does however have an advantage over less sophisticated filtering techniques as it accounts for system dynamics and generally provides strong performance.

CHAPTER 5

ILLINISAT ADACS ARCHITECTURE

5.1 Design Requirements

In order to produce a meaningful design, the system requirements must be thoroughly identified and discussed. By establishing design criteria, system performance may be evaluated. Furthermore it is critical to identify all design assumptions that are made so that the design may be modified in the future if the assumptions fail to hold.

The general goal of the IlliniSat program is to create a generic bus that is capable of supporting an array of scientific missions. This goal has a series of repercussions that must be identified.

First, as the ADACS system will be part of a generic bus that will be applied to a range of missions, not all mission specific requirements may be identified. This design must be flexible enough to support missions which are as of yet undefined. The ability to extend and adapt the current design to meet a varied range of missions must be considered throughout the design process.

Though specific mission requirements cannot be known beforehand, system requirements have been developed that will enable a range of missions to occur. Many scientific missions, such as remote sensing missions, require on-board, three-axis, active attitude control. To support this, accurate attitude knowledge, including angular rates, must be known throughout the mission.

All the requirements for the attitude determination system have been derived from requirements from the attitude control system. As developed in Reference [2], the requirements and constraints for the attitude control system are given in the table below.

Table 5.1: Attitude Control Requirements

Constraint	**Accuracy** (1-σ)
Pointing Accuracy	5° Per Axis
Worst Case Initial Spin	$5°/_{sec}$ Per Axis
Tracking Threshold	$0.1°/_{sec}$ magnitude

There are several considerations that went into the development of these constraints. The pointing accuracy constraint was developed in conjunction with the management of the IlliniSat program at the University of Illinois. This constraint was deemed appropriate to allow for the completion of the ION1 remote sensing mission, which would use photometers pointed in the nadir direction to study Oxygen chemistry in the upper

atmosphere. A system that meets this constraint would also be able to support a variety of other missions. The worst case initial tip off is based off of historical precedents for Cubesats. The tracking threshold is the point at which the satellite is no longer in the detumbling mode, which is the attitude control priority mode. In the tracking mode, the attitude control has been optimized to reject small torques and maintain a constant attitude with respect to the orbital reference frame.

With these constraints in mind, the following design goals have been established for the attitude determination system.

Table 5.2: Attitude Determination Requirements

Constraint	**Accuracy** (1-σ)
Pointing Knowledge	$< 0.5°$ Per Axis
Angular Rate Knowledge	$0.01°/_{sec}$ magnitude

These requirements were derived with the needs of the attitude control system in mind. Essentially, it is the goal of the attitude determination system to provide attitude knowledge to the attitude control system on the order of one order of magnitude below its requirements. This will allow the attitude control system to function within its designed parameters.

Next, the physical constraints of the ADACS system are of utmost importance. The IlliniSat must conform to the Cubesat specifications, so system volume, mass and power must be minimized. As part of the design of the IlliniSat bus, preliminary mass and power budgets have been established. These constraints are presented in the table below.

Table 5.3: ADACS Budget

Mass	75 g
System Power	300 mW
Peak Control Power	1.5 W

In addition to these constraints, the allotted volume for the electronics must be accounted for. All system electronics are integrated onto subsystem boards. These boards are 9 cm by 9 cm; boards are separated by 5 mm spacers. Thus, any electronic component must fit on the board and protrude no more than 2 mm from either side of the board (as electronic components may be mounted on both side of the board). Additionally, on board computational capacity is relatively limited as system processing is provided by an ARM9 processor. It is difficult to quantify the level of complexity that is acceptable, rather performance may be measured by system response time. The ADACS software calculations must be completed within one sampling period. The baseline sampling frequency has been set at 1 Hz.

Last, the definition of system error must be determined. Error will be described in terms of one standard deviation. This ensures that the system will perform within the given error margin 68% of the time. As noise is assumed to be normally distributed, any bias of the mean of the error will be resulting from insufficient number of data. Thus, any bias of the mean of the error will be ignored.

With the system requirements defined, the system design can be presented in a meaningful light.

5.2 Attitude Determination Design Concept

There are several considerations to be taken into account when developing an attitude determination system. The decision whether to directly measure the attitude state or to use an algorithm to infer the current state must be made.

Within the IlliniSat program, work has been done on designing a system that uses only magnetic field measurements to determine the full state by using an extended Kalman filter. This technique is proposed in Reference [5]. However, as discussed in Reference [3], there are a number of problems with this technique. Foremost, the filter tends to diverge. This is due to the fact that the nonlinear dynamics are not strongly observable given the two measurable attitude components from a three-axis magnetometer. Further, Reference [5] makes the assumption that spacecraft is gravity gradient stabilized and nadir pointing. This assumption confines the initial attitude to be nominally nadir pointing, which is not necessarily the case for IlliniSat. It is likely that the problems encountered with determining the full state from magnetometer measurements is due to the low level of observability of the dynamics.

The alternative to this method is to increase the number of sensors on the satellite so that the attitude and angular rates are more readily observable. Given two separate vector measurements in the satellite body frame as well as their reference values in the inertial frame, the attitude may be directly measured. From here, several techniques may be employed to improve attitude knowledge accuracy. Additionally, angular rate information may be supplied by rate gyros or through the use of an algorithm.

Further, the degree and nature of noise reduction techniques must be explored. In many cases when both the attitude and angular rates are being estimated, an extended Kalman filter is employed. However, this filter is not an optimal estimator. By examining Equation 3.25, one notices that the attitude dynamics are linear, assuming the angular rates are known. However, the dynamics of the angular rates, as shown in Equation 3.24, are nonlinear. Yet, by separating the estimation of the angular rates from the estimation of the attitude, the system may be simplified. By doing this, a linear Kalman filter may be used for estimating attitude (which is an optimal filter), while an extended Kalman filter may be used to estimate the angular rates. Given these ideas, a definitive system concept may be defined.

5.3 Attitude Determination System Overview

Given the constraints and aspirations detailed in the above section, a detailed system was designed. To simplify the system, the task of determining angular rates was separated from the task of determining the attitude.

Several options for determining angular rates were explored. First, rate gyros may be used. There are commercially available, micro electromechanical (MEMS) gyroscopes available. These sensors directly measure the angular rates. These devices are often low powered, low mass and relatively small. The second option that was explored was to use an algorithm to determine the angular rates from the vector measurements provided by other on board sensors. Both of these techniques were modeled and are presented in Chapter 6.

After measuring the angular rates, either directly or through manipulation of other sensor data, several techniques to mitigate system noise may be employed. As cubesats historically are deployed with low angular rates, noise may be reduced in several manners. A moving average filter may be used as these are effective for reducing noise on quantities that are constant or slowly changing. An extended Kalman filter may also be used to reduce noise. This technique makes use of the known system dynamics as well as the statistical distribution of noise in the measurement. Both of these techniques are explored in Chapter 6.

Last, the attitude must be determined. Given the decision to have the ability to directly measure the attitude, at least two sensors that measure a known vector are needed. The sensor used previously within the IlliniSat program were a three axis magnetometer as well as a coarse sun sensor. Both of these sensors allow the system to measure known vector quantities while maintaining system simplicity. Thus, there is no reason to change the sensor suite. Given two measurements of vector quantities within the satellite body frame, as well as the knowledge of those vectors in the inertial frame, the attitude may be directly computed. From here, a linear Kalman filter may be used to reduce system noise. This technique is simulated in Chapter 6. Figure 5.1 presents a flow chart of the attitude determination concept.

5.4 Attitude Determination System Hardware Details

The attitude determination sensors have been explored throughout the IlliniSat program. Several candidates for rate gyros have been identified. The primary design driver for the rate gyros is to provide accurate measurements while maintaining low power and size requirements. Earlier in the program, it has been difficult to obtain commercially available rate gyros that meet these requirements. Specifically, MEMS gyros have historically only provided yaw rate information, necessitating the gyros to be mounted orthogonally to each other, requiring a larger amount of space. However, *Invensense*, a MEMS sensor developer, has produced a range of MEMS gyros that measure pitch, roll and yaw rates [11]. As they do not manufacture a three axis rate gyro, two separate gyros are needed. As further hardware testing is necessary to determine the performance characteristics, several candidate rate gyros have been identified.

There are two gyros listed in Table 5.4 that give the yaw rate information. This is because it may be useful to have one redundant axis of rate information. Depending on the noise characteristics and sensor drift, an additional axis of information may prove useful to improve accuracy. If this is not required, only a the single yaw gyro shall be used.

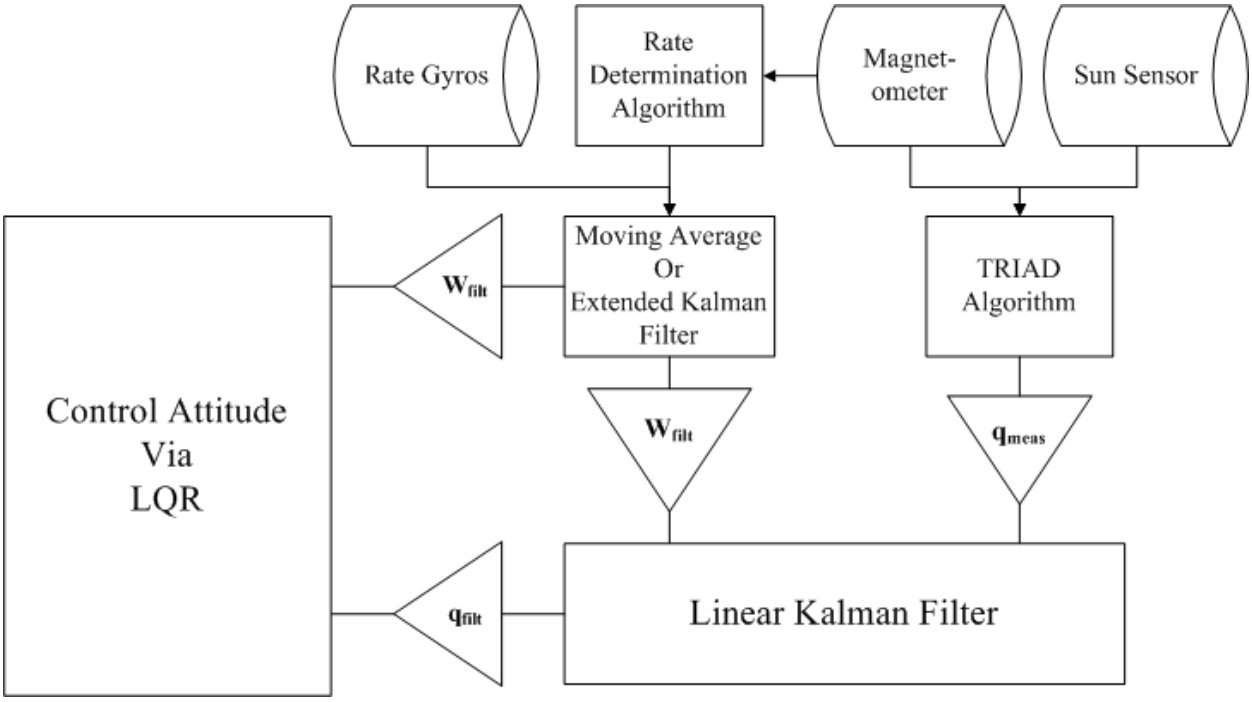

Figure 5.1: Attitude Determination Concept

Table 5.4: Invensense Rate Gyro Characteristics

Part Number	**Measurement Axis**	**Range** [$\pm°/_{sec}$]	**Size** [mm]	**Power** [mW]
IDG-1215	Pitch and Roll	67	4x5x1.2	21
ISZ-1215	Yaw	67	4x5x1.2	13.5
IXZ-500	Pitch and Yaw	110	4x5x1.2	19.5

In order to integrate these analog sensors within a digital system, an analog to digital converter (ADC) must be used. When choosing this device, the signal must be sufficiently discretized such that the voltage step at the desired sensitivity may be measured. The lowest discrete step that can be measured by the ADC is known as the Least Signficant Bit (LSB) value. These considerations are summarized in Table 5.5. By chosing a 16 bit ADC, the output of the rate gyros may be sample to enough sensitivity so that an increment of 0.01 $°/_{sec}$ may be measured. Though the device may be measured to this sensitivity, system noise will still be present.

The magnetometer must also be a low powered device. *Honeywell* manufactures a range of magnetometers. Through the course of the IlliniSat program, one sensor has been chosen due to its low power use as well as

Table 5.5: Rate Gyro Sensitivity Considerations

Part Number	**Output Scale** [$mV/°/_{sec}$]	**Required Bit Level**	**LSB** [$°/_{sec}$]
IDG-1215	15	14	0.0082
ISZ-1215	15	14	0.0082
IXZ-500	9.1	16	0.0034

its integrated digital interface. Table 5.6 lists the characteristics of this sensor.

Table 5.6: Honeywell Magnetometer Characteristics

Part Number	**Sensitivity [μ Gauss]**	**Range [$\pm$Gauss]**	**Size [mm]**	**Power [mW]**
HMC6343	85	2	9x9x1.9	14.9

There are several options for a sun sensor. The simplest option is use the solar panels as a coarse Sun sensor. As the output voltage of a solar panel is a function of the incidence angle of Sun's radiation, by measuring the output voltage of the panels, the location of the Sun in the body frame may be triangulated. At this point, specific hardware for the Sun sensor has not been chosen in the IlliniSat program.

5.4.1 Angular Rate Extended Kalman Filter Derivation

It is anticipated, based on historical precedent for nano-satellites, that the angular rates remain quite low. Furthermore, due to the scale of the satellite, large torques are generally not present. Therefore, the angular rates tend to change slowly. These characteristics allow for noise removal to be performed by a moving average, as this scenario is where they excel. However, as all the mission needs for a generic bus cannot be identified prior to their formulation, an EKF for the angular rates may prove useful.

For this algorithm, it is assumed that the angular rates may be measured, either directly with rate gyros, or through processing other sensor data to recover the angular rates. Either process will include an amount of sensor noise that will need to be removed.

To reiterate, the dynamics for the angular rates are as follows.

$$\dot{\omega}^{B/I} = \tilde{I}^{-1}\left(\tau - \omega^{B/I} \times (\tilde{I}\,\omega^{B/I})\right) \tag{5.1}$$

This process is clearly non-linear, so a standard Kalman filter cannot be used. However, an extended Kalman filter is able to handle non-linear dynamics. First, the equation propagating the dynamics forward in time must be written. The simplest method for accomplishing this is using the standard forward-Euler propagation.

$$\omega_k \simeq \omega_{k-1} + \dot{\omega}\,dt \tag{5.2}$$

Since the angular rates are the quantity that is of interest, the state for this filter will be the angular rates.

$$\mathbf{x} = \omega \tag{5.3}$$

The update equation is then the forward Euler approximation, which is as follows.

$$\hat{\mathbf{x}}_k^- = \hat{\mathbf{x}}_{k-1}^- + \dot{\mathbf{x}}_{k-1}\,dt \tag{5.4}$$

So now, the Jacobian matrix of the derivatives of Equation 5.2 with respect to the state must be calculated.

$$\begin{aligned} A &= \frac{\partial \mathbf{f}}{\partial \mathbf{x}} \\ &= \tilde{I}^{-1} \begin{bmatrix} J_{11} & J_{12} & J_{13} \\ J_{21} & J_{22} & J_{23} \\ J_{31} & J_{32} & J_{33} \end{bmatrix} \end{aligned} \tag{5.5}$$

Where $J_{i,j}$ is given by the following.

$$\begin{aligned} J_{11} &= \tilde{I}_{1,3}\hat{x}_2^- - \tilde{I}_{1,2}\hat{x}_3^- \\ J_{12} &= \tilde{I}_{1,3}\hat{x}_1^- + 2\tilde{I}_{2,3}\hat{x}_2^- + \tilde{I}_{3,3}\hat{x}_3^- - \tilde{I}_{2,2}\hat{x}_3^- \\ J_{13} &= \tilde{I}_{3,3}\hat{x}_2^- - \tilde{I}_{1,2}\hat{x}_1^- - \tilde{I}_{2,2}\hat{x}_2^- - 2\tilde{I}_{2,3}\hat{x}_3^- \\ J_{21} &= \tilde{I}_{1,1}\hat{x}_3^- - 2\tilde{I}_{1,3}\hat{x}_1^- - \tilde{I}_{2,3}\hat{x}_2^- + \tilde{I}_{3,3}\hat{x}_3^- \\ J_{22} &= \tilde{I}_{1,2}\hat{x}_3^- - \tilde{I}_{2,3}\hat{x}_2^- \\ J_{23} &= \tilde{I}_{1,1}\hat{x}_1^- + \tilde{I}_{1,2}\hat{x}_2^- + 2\tilde{I}_{1,3}\hat{x}_3^- - \tilde{I}_{3,3}\hat{x}_1^- \\ J_{31} &= 2\tilde{I}_{1,2}\hat{x}_1^- + \tilde{I}_{2,2}\hat{x}_2^- + \tilde{I}_{3,3}\hat{x}_3^- - \tilde{I}_{1,1}\hat{x}_2^- \\ J_{32} &= \tilde{I}_{2,2}\hat{x}_1^- - \tilde{I}_{1,1}\hat{x}_1^- - 2\tilde{I}_{1,2}\hat{x}_2^- - \tilde{I}_{1,3}\hat{x}_3^- \\ J_{33} &= \tilde{I}_{2,3}\hat{x}_1^- - \tilde{I}_{1,3}\hat{x}_2^- \end{aligned} \tag{5.6}$$

The noise covariance matrix and the Kalman gain are given as follows

$$P_k^- = A_k \, P_{k-1} \, A_k^T + Q \tag{5.7}$$

$$K_k = P_k \, \left(P_k + R\right)^{-1} \tag{5.8}$$

Then finally, the state update and covariance update can be expressed by the following equations.

$$\hat{\mathbf{x}}_k = \hat{\mathbf{x}}_k^- + K_k \left(\omega_{measured} - \hat{\mathbf{x}}_k^-\right) \tag{5.9}$$

$$P_k = \left(I_{3x3} - K_k\right) \, P_k^- \tag{5.10}$$

In this process the process noise and measurement noise covariance matrices may not be easily calculated. One method for finding these matrices is using an optimizer such as a genetic algorithm or synthetic annealing. Typical system noise may be modeled and the optimizer can be used to find the matrix values that minimize the error in the estimate. These matrices are positive definite and are generally diagonal assuming that noise is independent on each axis.

Using this technique, the angular rates may be more accurately estimated.

5.4.2 Quaternion Kalman Filter Derivation

This algorithm uses the filtered angular rates as well as the measured attitude as an input. In order to increase the accuracy of the attitude knowledge, a Kalman filter may be used. If one examines Equation 3.25, it can be seen that if the angular rates have been determined, than the attitude dynamics become linear. This is useful as the Kalman filter is an optimal linear estimator.

The derivation of the Kalman filter in this situation is simple. The state in this case will be the attitude quaternion. Given that the attitude may be measured directly at any time, the equations of the Kalman filter are simplified. First the state is propagated forward in time given the dynamics; however, as determination will only take place when the system is not being controlled the equation is simplified.

$$\hat{\mathbf{x}}_k^- = A\hat{\mathbf{x}}_{k-1} \tag{5.11}$$

$$P_k^- = A\,P_{k-1}\,A^T + Q \tag{5.12}$$

Here, A is given by the state transition matrix specified in Equation 3.29. From there, the estimate is updated with the current measurement. As the attitude quaternion can be measured, the measurement matrix H becomes the identity matrix.

$$\hat{\mathbf{x}}_k = \hat{\mathbf{x}}_k^- + K_k\,\left(\mathbf{z}_k - \hat{\mathbf{x}}_k^-\right) \tag{5.13}$$

$$P_k = (I - K_k)\,P_k^- \tag{5.14}$$

The optimal gain K is given by the following equation.

$$K_k = P_k^-\left(P_k^- + R\right)^{-1} \tag{5.15}$$

Again, the noise and process covariance matrices are not explicitly known, but may be calculated as before with an optimizer. It should be noted that an error in the angular rates will contribute to the process error. Given this filter, the minimum variance estimate of attitude can be made.

5.4.3 Attitude Control Summary

The main contribution of this thesis is in the development of the attitude determination algorithms. However, for completeness, the attitude control theory will be summarized. For an in depth development of this concept, refer to Reference [2].

Active control of IlliniSat is provide by three electromagnets. These magnetic torque coils are simple devices; a magnetic dipole is created by generating a current through concentric loops of wire. As these torque coils interact with the Earth's magnetic field, a torque is generated.

After determining the current axis, a control law may be applied to provide active three axis control of the satellite. Linear Quadratic Regulator (LQR) theory is used to develop an optimal control. LQR theory begins with the standard linear dynamics.

$$\dot{\mathbf{x}} = A\,\mathbf{x} + B(t)\,\mathbf{u} \tag{5.16}$$

From here, a cost functional is defined.

$$J = \frac{1}{2}\int_{t_0}^{t_f} \left(\mathbf{x}^T Q\mathbf{x} + \mathbf{u}^T R\mathbf{u}\right) dt + \frac{1}{2}\mathbf{x}(t_f)^T P\mathbf{x}(t_f) \tag{5.17}$$

This cost functional can be thought of as assigning a cost for several factors. The cost associated with deviation from the desired state over the range of time is weighted by the Q matrix, while the cost associated with the use of control is weighted by the R matrix. The cost with deviation from the final state is weighted by the P matrix. All of these matrices are constant and may be adjusted by the design to favor various aspects of performance. In practice, a genetic algorithm may be used to calculate the optimal matrix values given more specific design goals, such as minimize power use for control.

This problem has a well known solution. Yet, given the fact that an orbiting satellite will experience a periodic magnetic environment an additional simplification may be made. In this case an asymptotic periodic linear quadratic regulator can be used, as the control matrix B is periodic. Given this simplification, the optimal control is given by the following equation.

$$\mathbf{u}^\circ = -R^{-1}\,B(t)^T\,P_{ss}\,\mathbf{x} \tag{5.18}$$

This calculation of the optimal control is computationally less complex as the matrix P_{ss} is not time varying, as is the case for the LQR. In fact, this matrix may be calculated *a priori* given a nominal orbit. The P_{ss} is given by solving the following matrix Riccati equation.

$$Q + P_{ss}\,A + A^T\,P_{ss} - P_{ss}\,C\,P_{ss} = \mathbf{0} \tag{5.19}$$

Here, the matrix C is given by the following.

$$C = \frac{1}{15\tau}\int_0^{15\tau} B(t)\,R\,B(t)^T\,dt \tag{5.20}$$

Now, the state being controlled can include the attitude, the integral of the attitude as well as the angular rates. This has the added benefit of minimizing steady-state error, providing increased stability as well as

reducing the effects of system noise. The state may then be defined in the following manner.

$$\tilde{\mathbf{x}} = \begin{bmatrix} \int \mathbf{q}^{B/R} \\ \mathbf{q}^{B/R} \\ \omega^{B/R} \end{bmatrix} \tag{5.21}$$

It must be noted here that the attitude is expressed with respect to the orbital reference frame, not the inertial frame. So, the attitude must be converted to be in the proper reference frame. Given this state, the dynamics are then as follows.

$$\tilde{\mathbf{x}} = \tilde{A}\,\tilde{\mathbf{x}} + \tilde{B}\,\mathbf{u} \tag{5.22}$$

Where the modified matrices are as follows.

$$\tilde{A} = \begin{bmatrix} \mathbf{0} & I \\ \mathbf{0} & A \end{bmatrix} \tag{5.23}$$

$$\tilde{B} = \begin{bmatrix} \mathbf{0} \\ \mathbf{0} \\ -\tilde{I}\,S(\mathbf{b}(\mathbf{t})) \end{bmatrix} \tag{5.24}$$

Here, the operator S is given by the following.

$$S(\mathbf{b}) = \begin{bmatrix} 0 & -b_3 & b_2 \\ b_3 & 0 & -b_1 \\ -b_2 & b_1 & 0 \end{bmatrix} \tag{5.25}$$

Given these equations, the optimal control can be calculated.

CHAPTER 6

SIMULATION RESULTS

6.1 System Simulator Description

In order to test the attitude determination and control system, a full simulator was constructed using MATLAB. This simulator was constructed as part of the IlliniSat project and made use of previously developed control code. As this is a complex system, a conceptual diagram is depicted in Figure 6.1.

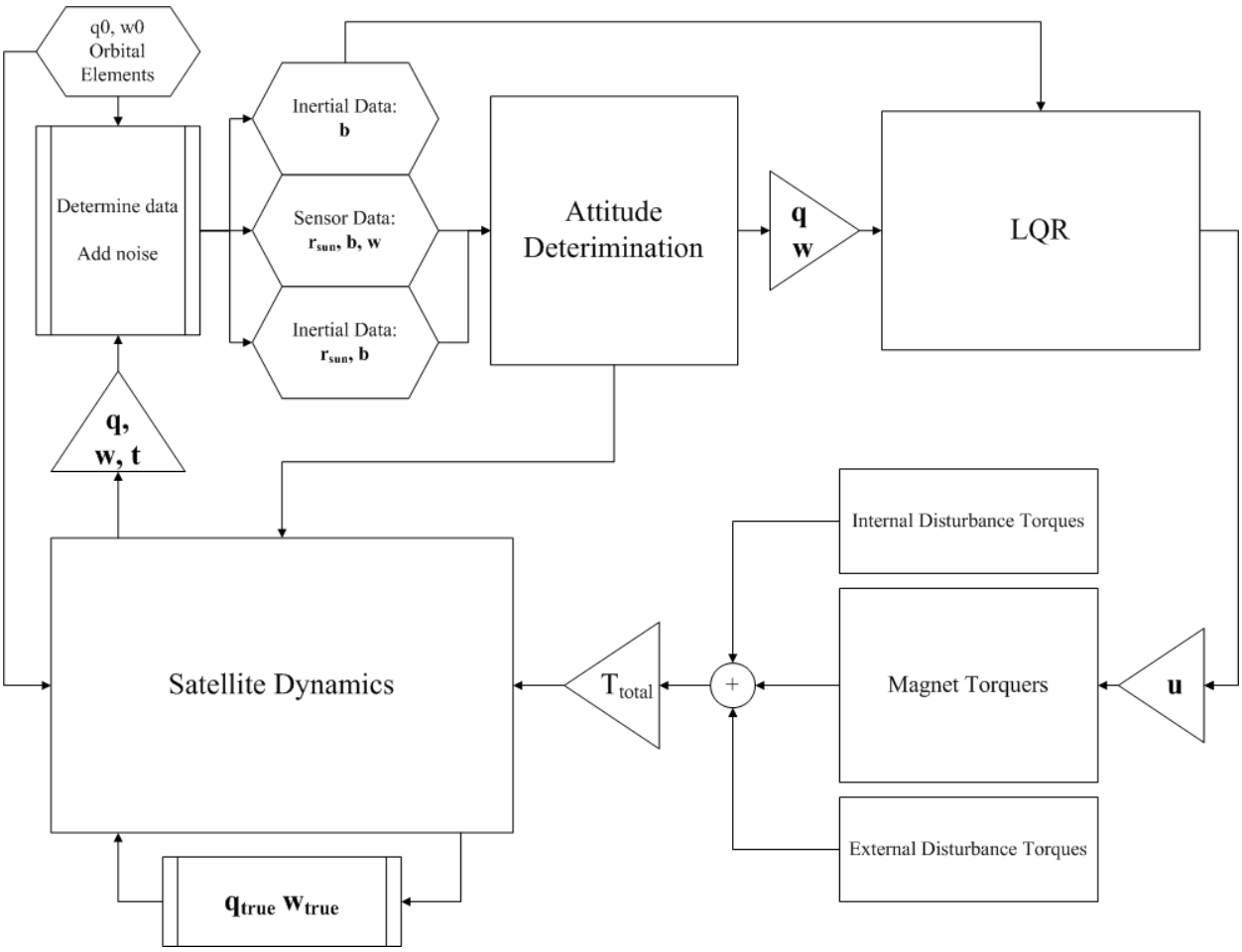

Figure 6.1: ADACS Simulator Concept

The simulator has initial conditions of initial attitude, initial angular rates, the orbital elements as well as the epoch time. This information is used to propagate both the current position of the satellite as well as the attitude and angular rates forward in time. Given the current position and attitude, all the necessary sensor information can be simulated. The attitude determination algorithm requires the position of the sun and the magnetic field vector in the Earth inertial reference frame. This algorithm also requires simulated sun position, magnetic and angular rate vectors in the satellite body frame. These vectors also contain simulated noise. From here, the determined attitude, angular rates and the magnetic field vector in the inertial frame are input to the control algorithm, the LQR. This calculates the optimal control given these inputs. It should be noted that the control block uses the quaternion that is defined with respect to the orbital frame rather than the inertial frame. This necessitates a coordinate transform. Given the calculated optimal control, the torque produced given the current magnetic field is then calculated. There are also blocks to determine disturbance torques from external sources, such as drag and gravity gradient, as well as internal sources, such as unintended magnetic torques. Currently, no internal disturbance torques are modeled. The total torque on the satellite is then given as an input to the satellite dynamics block. The state of the satellite is propagated forward in time and the process is then repeated.

Given that hardware testing has yet to be completed, several noise conditions were examined when testing the attitude determination software. This noise level is summarized in Table 6.1

Table 6.1: Sensor Noise

Sensor	**Nominal Noise**	**Surplus Noise**
Magnetometer	200 nT	1800 nT
Sun Sensor	7% of full scale	14% of full scale
Rate Gyro	$0.1°/_{Sec}$	$0.2°/_{Sec}$

This noise specifies the variance of the measurement and was applied on each axis. The nominal magnetometer noise is based off the value specified on the data sheet of HMC6343 magnetometer. The surplus noise value is based off of the experimentally measured noise value. As this noise level is much higher than expected, it is most likely due to environmental factors during testing and is currently being explored. However, this value is simulated so that the effectiveness of the attitude determination scheme can be demonstrated even in the presence of high noise. The nominal Sun sensor noise corresponds to a 10° accuracy of each sensor. This calculation was completed as part of a simulation in the IlliniSat project. This also corresponds to roughly twice the angular resolution given by Reference [12] for a coarse Sun sensor. The surplus noise is then twice this noise level to simulate poor sensor performance. Finally, the rate gyro nominal noise level is given as twice the specified value in the IDG-1215 data sheet. The surplus noise is again twice this value. These noise levels offer conservative estimates on what will be experienced in flight and will envelope any extraneous noise sources.

Given these noise values, the attitude and rate Kalman filters may be optimized. The Simulated Annealing (SA) optimizer was used to find optimal values for the measurement and process noise covariance matrices.

SA uses a random walk process to minimize an objective function; which in this case was the total standard deviation of the error. The optimizer was run for a range of initial conditions for tumbling and tracking angular rates at nominal and surplus noise values. It must be noted that as hardware testing progresses and noise measurements are refined, the noise matrices must be updated.

All of the test cases were run with a typical reference orbit. The circular orbit has an inclination of 45° and an altitude of 500 km. At the epoch of June 28^{th}, 2010, the argument of perigee, the true anomaly and the right ascension of the ascending node are zero.

With the system simulator developed, each filter's performance may be measured by itself. As the angular rates are an input to the attitude filter, the rate filter must be characterized by itself first. Then, after its performance is established, the attitude filter's quality may be attained. Once the attitude determination system has been characterized, then the full system's capabilities may be described.

6.2 Angular Rate Determination

Several scenarios were simulated for angular rate determination. First, both a simple moving average and an extended Kalman filter were examined assuming angular rates could be measured. Error calculations were made for initial conditions at both detumbling and tracking rates at both levels of noise. In addition, the algorithm for calculating angular rates based on one vector measurement was examined.

6.2.1 Rate Gyro Simulation

A simulation was conducted assuming angular rate information could be sample from a three-axis rate gyro. Nominal and surplus noise levels were examined at both tracking and tumbling angular rates. The results for the nominal noise levels will be discussed first. Table 6.2 gives the initial conditions for each case.

Figure 6.2 and Figure 6.3 compare the noisy measurement, the output from the Kalman filter and the simple moving average (SMA) to the true angular rates. Notice that due to the fact that the satellite is axis-symmetric, the ω_3 value does not vary as much as ω_1 and ω_2 in the first figure. It shows that when angular rates are lower, the SMA does a reasonable job of filtering noise; however, at higher angular rates, the SMA consistently lags the true value. The Extended Kalman Filter (EKF) performs well in both cases.

Table 6.2: Angular Rate Initial Conditions

$\omega_{\mathbf{Tumbling}}$	$[5 \ -.5 \ 5]^T$
$\omega_{\mathbf{Tracking}}$	$[-.08 \ -.95 \ .07]^T$

Both cases were then simulated at above nominal noise levels. Error was calculated in all cases as the difference between the true value and the filtered or smoothed value. The standard deviation of the error for the angular rate EKF is given in Table 6.3.

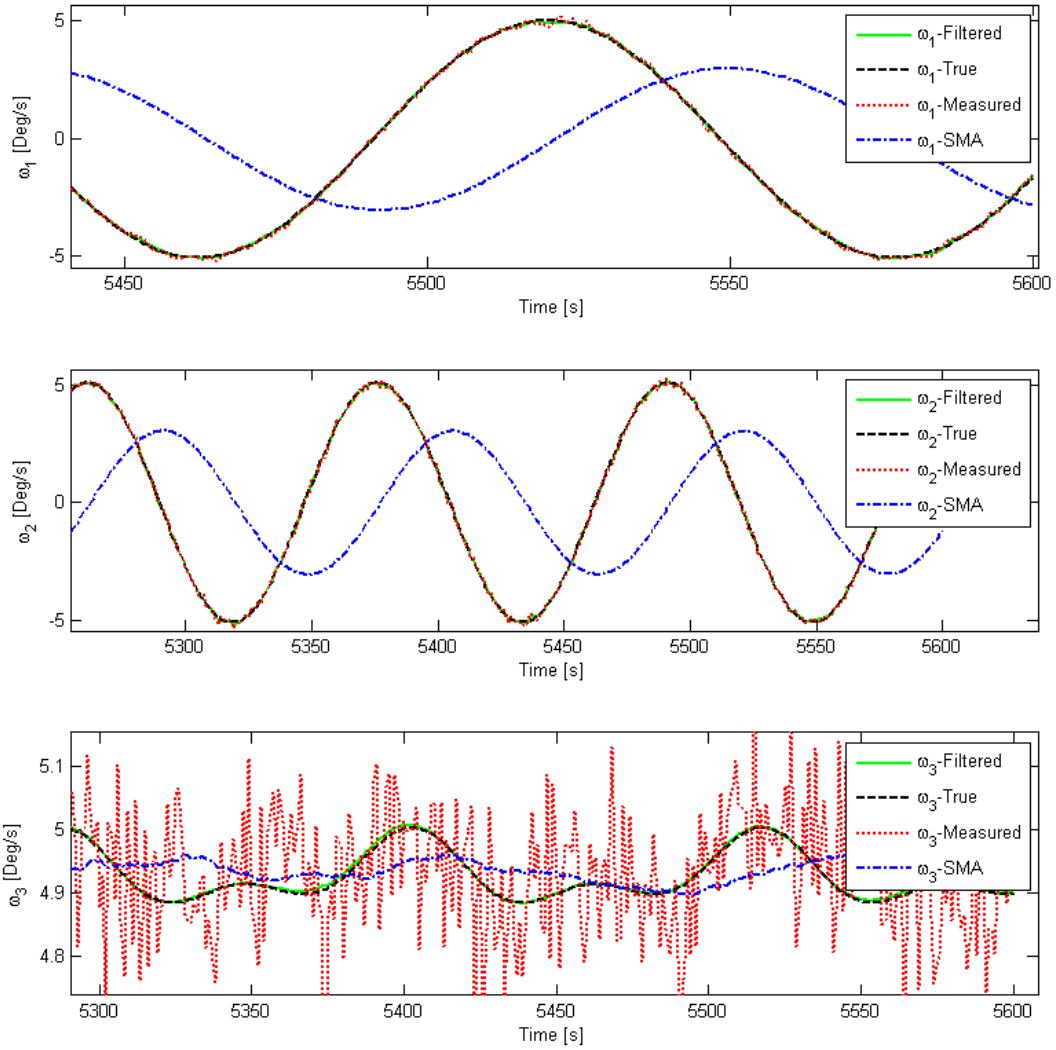

Figure 6.2: Tumbling Angular Rate Simulation With Rate Gyros Given Nominal Noise and High Rates

Table 6.3: EKF Simulation Error Standard Deviation Summary

Initial Condition	**Noise Level**	$\omega_1[^\circ/_{Sec}]$	$\omega_2[^\circ/_{Sec}]$	$\omega_3[^\circ/_{Sec}]$
Tracking	Nominal	0.009340	0.01140	0.005415
Tracking	Surplus	0.02447	0.01938	0.03714
Tumbling	Nominal	0.04225	0.04567	0.007834
Tumbling	Surplus	0.06324	0.06926	0.06587

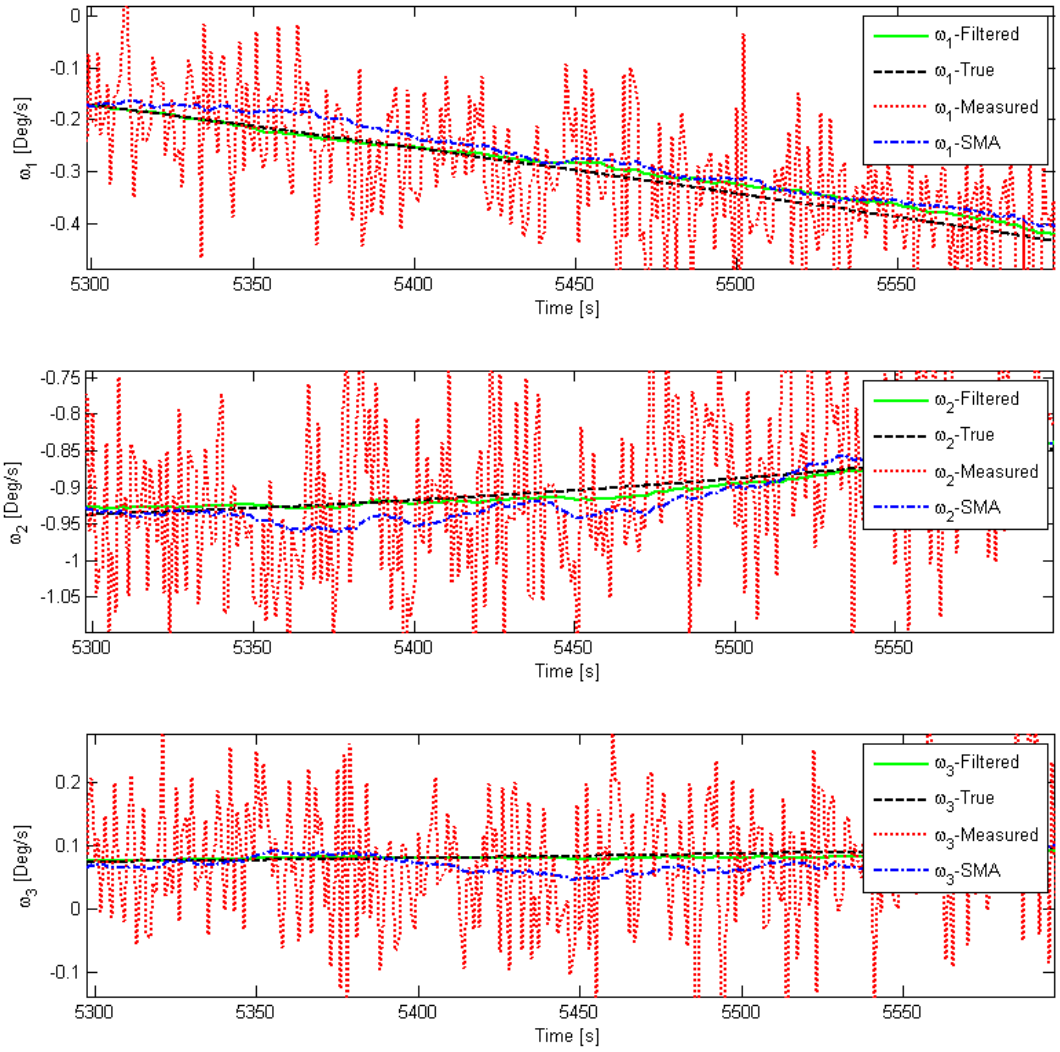

Figure 6.3: Tracking Angular Rate Simulation With Rate Gyros Given Nominal Noise and Low Rates

It can be seen that even for high noise levels, the EKF performs quite well. The SMA has an average error that is much higher in all cases.

6.2.2 Angular Rate Determination From Vector Measurements

Next, the method outlined in Section 4.2 was implemented. By observing successive vector measurements, the angular rates may be estimated. In order to show the concept is feasible, two trial cases were run. The first case was run without sensor noise and with a diagonal moment of inertial matrix where $I_1 = I_2 = I_3$ using measurements from the Sun sensor. Figure 6.4 shows a three dimensional plot of the angular velocity vector. A three dimensional plot is used here as it gives insight into how the algorithm functions. As the moment of inertia matrix is diagonal, the angular velocity remains a fixed point. As can be seen, the estimation given by the algorithm is within $0.05°/_{sec}$ with the actual angular velocity being $[5 \quad -0.5 \quad 5]^T$.

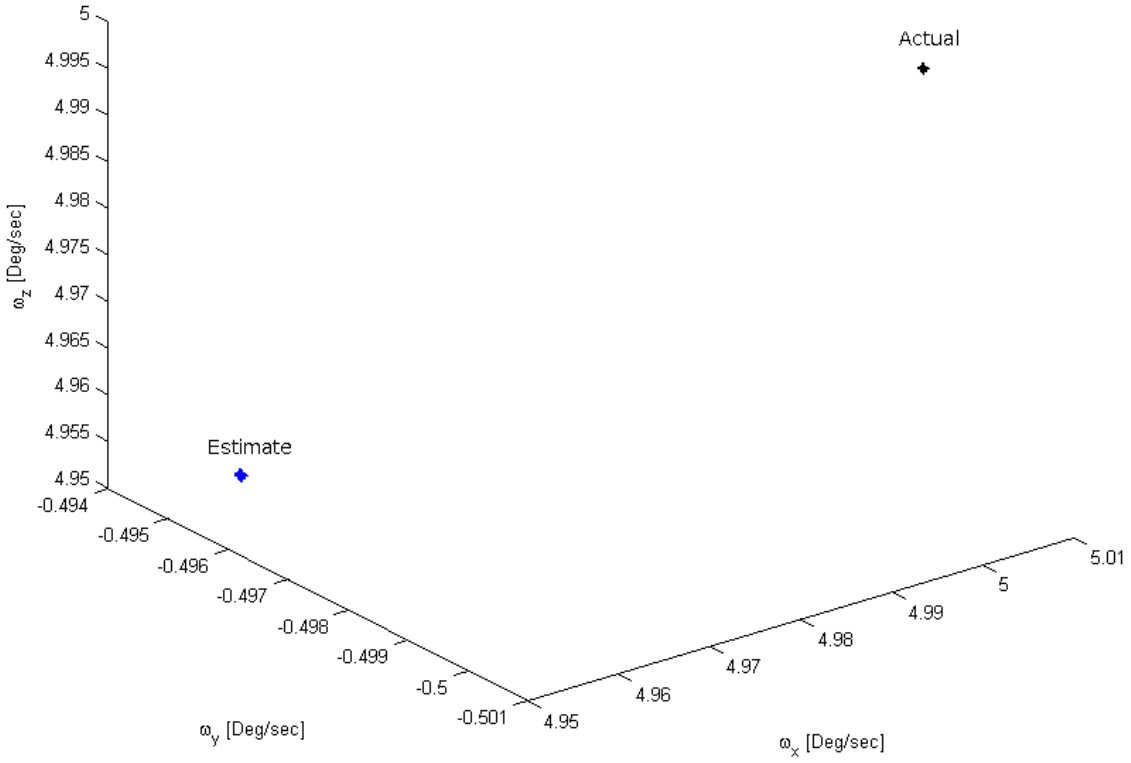

Figure 6.4: Angular Rate Estimate From Vector Information With Diagonal Moment of Inertia

The next test case that was run was with no sensor noise and with a moment of inertia matrix where $I_1 = I_2 > I_3$. This test case demonstrates strange behavior. As can be seen, the angular rates determined by the algorithm periodically vary from the true value. The motion of this observation resembles the motion on the body of a precessing top. Reference [13] discusses such motion. Figure 6.5 shows this result. This moment of inertial matrix causes the body to rotate with a coning motion. This coning then affects the estimation process from this algorithm. As can be seen, this causes a biased error of nearly $0.6°/_{sec}$. This result is unacceptable as it is much higher than the requirement discussed in Table 5.2. Furthermore, as this error is biased —not normally distributed— a Kalman filter is unable to mitigate this noise.

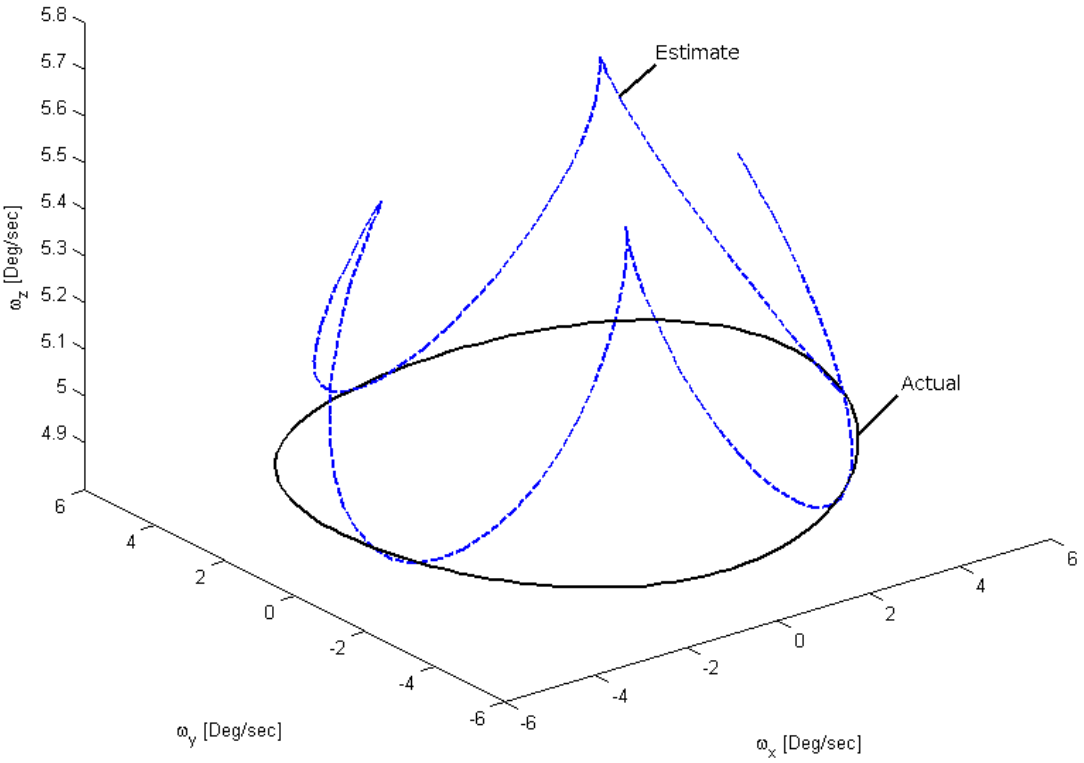

Figure 6.5: Angular Rate Estimate From Vector Information With Actual Moment of Inertia

The last test case was run using the true moment of inertial matrix and with the nominal sensor noise value for the Sun sensor. This algorithm is sensitive to noise; the resulting rate estimation has a high degree of error. The output of this algorithm was filtered with an EKF, but the results had an average error of $6°/_{sec}$. As the output has a high amount of noise, it is not informative. Figure 6.6 shows the root mean

square (RMS) error for the simulation for both the measured output and the filtered output.

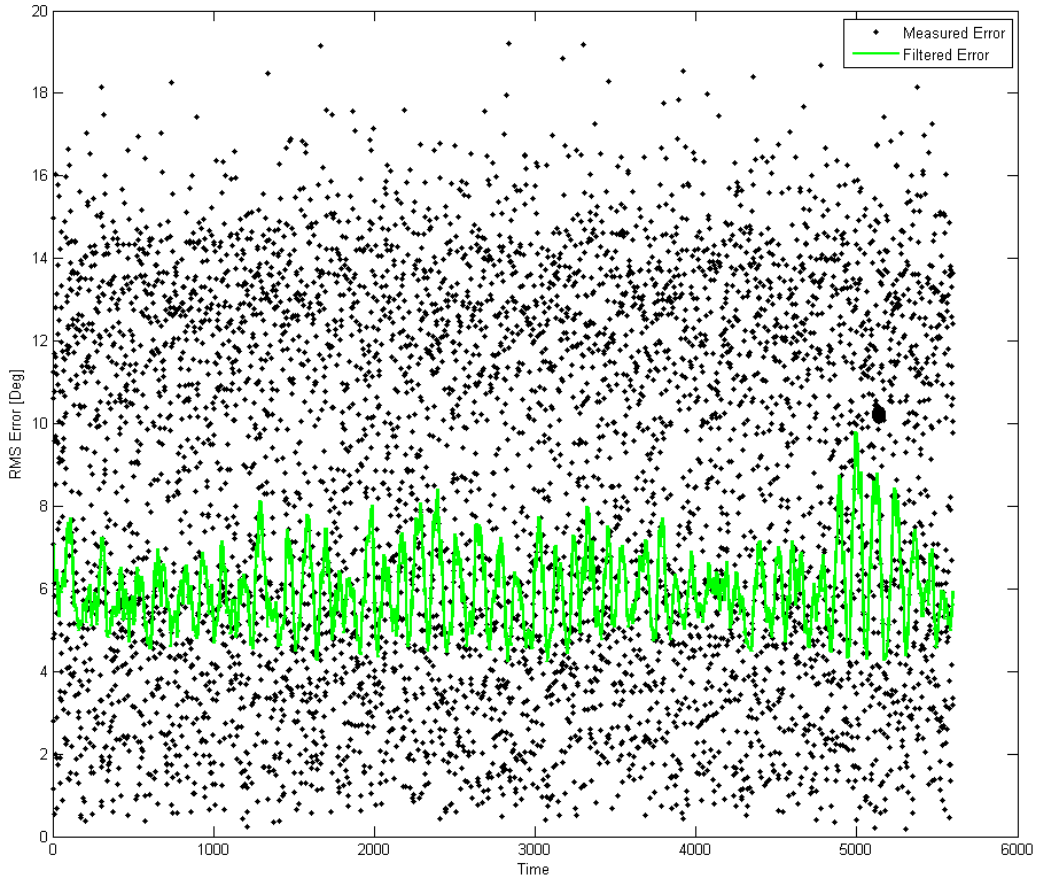

Figure 6.6: RMS Error For Measured and Filtered Angular Rate Output Using Sun Sensor Vector Measurements With Nominal Noise Values

As can be seen, the angular rate determination from vector observations does not provide the necessary level of accuracy to achieve the control goals.

6.3 Attitude Determination

Once the angular rates have been determined and have been smoothed, the attitude can be determined. This simulation was conducted assuming that the angular rates were smoothed with the EKF as it provided the most accurate results. The same test cases were run for the attitude filter, with the same initial conditions for the angular rates. The initial attitude quaternion was $[0 \;\; 0 \;\; 0 \;\; 1]^T$.

The first test condition was determining the attitude during tumbling given nominal noise. Figure 6.7 shows the measured attitude, the filtered output as well as the true values of the attitude quaternion for a

representative time period of one orbit. Figure 6.8 shows the error in the roll, pitch and yaw angles over one orbit, while Figure 6.9 shows expanded detail of that figure over a representative time period. Notice the one standard deviation is marked on both figures.

The second test case that was run was for nominal noise but with the slower angular velocities associated with tracking. Again the attitude filter is able to reject a large amount of noise and track the true dynamics. Figure 6.10 depicts the attitude output for a typical time frame in one orbit. Next, Figure 6.11 depicts the error in the pointing knowledge for a typical time frame during one orbit. Notice the typical error for the roll, pitch and yaw angle knowledge is nearly zero.

Further test cases were conducted given the surplus noise condition. These figures closely resemble the figures for the other test cases, and have been omitted. The resulting error distribution for all test cases are summarized in Table 6.4.

Table 6.4: Attitude Kalman Filter Simulation Error Deviation Summary

Initial Condition	**Noise Level**	Roll Error [°]	Pitch Error [°]	Yaw Error [°]
Tracking	Nominal	0.4672	0.7714	0.3864
Tracking	Surplus	1.273	1.602	1.316
Tumbling	Nominal	0.7578	0.7054	0.8140
Tumbling	Surplus	1.240	1.270	1.164

Simulation results show that given nominal noise and a range of initial conditions, the attitude determination system is able to maintain error standard deviation under 1°. Given larger amounts of noise, the knowledge error standard deviation is maintained well below 2°.

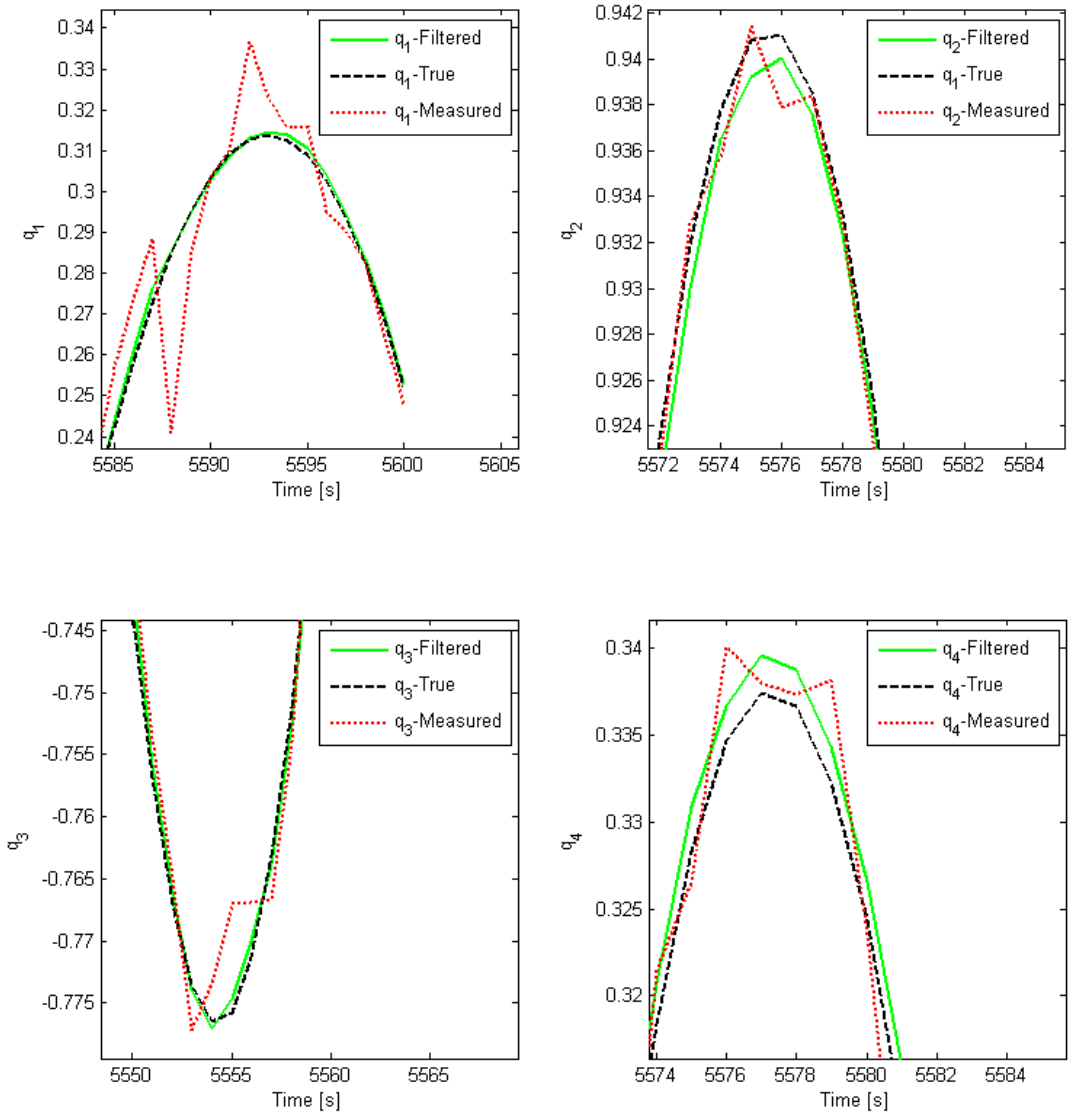

Figure 6.7: Measured and Filtered Attitude Given Nominal Noise and Tumbling

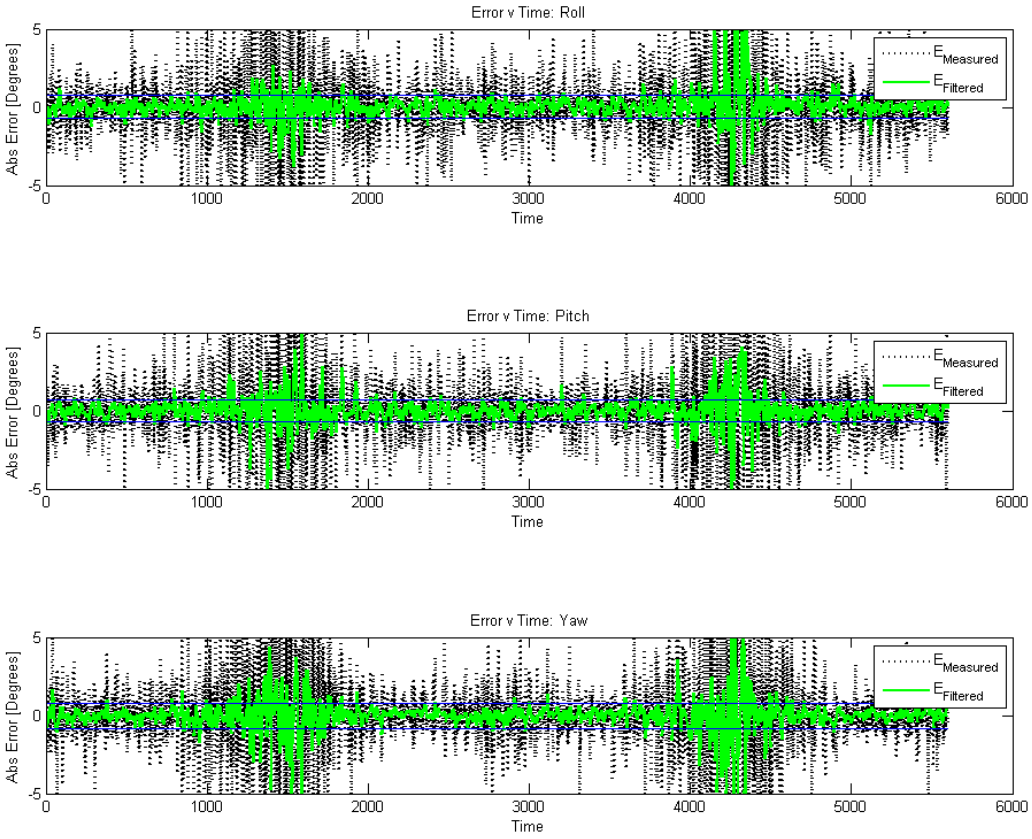

Figure 6.8: Pointing Knowledge Angular Error For One Orbit Given Nominal Noise and Tumbling

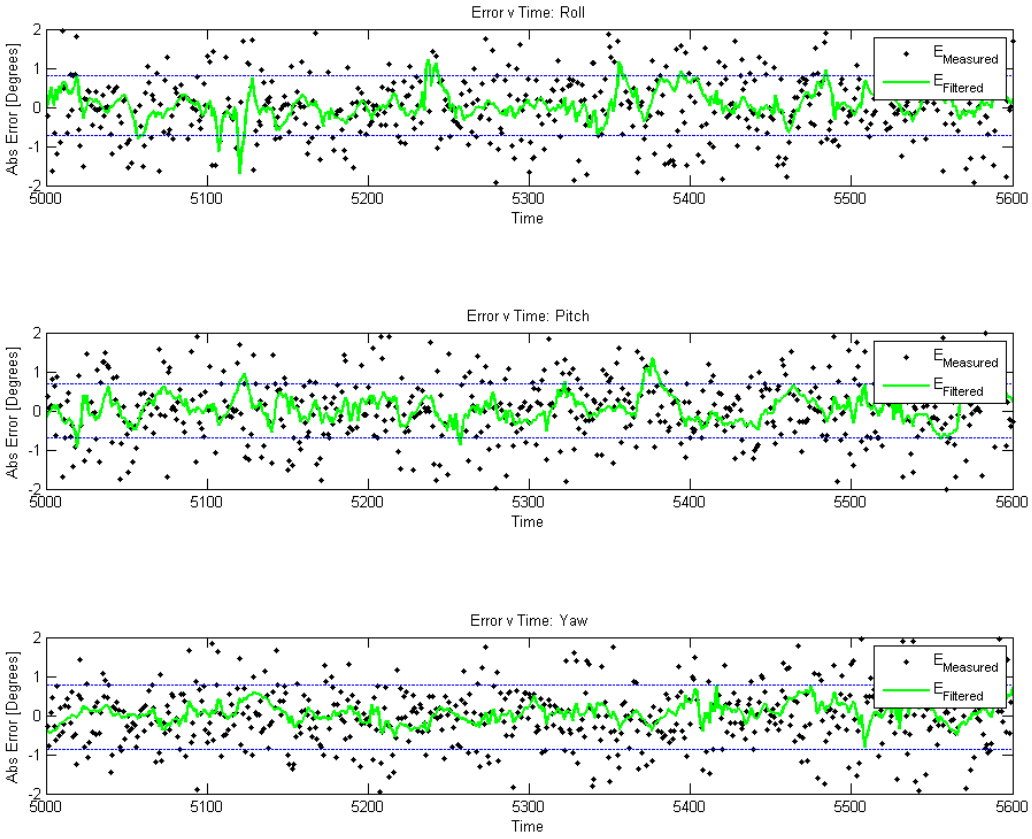

Figure 6.9: Refined Pointing Knowledge Angular Error For One Orbit Given Nominal Noise and Tumbling

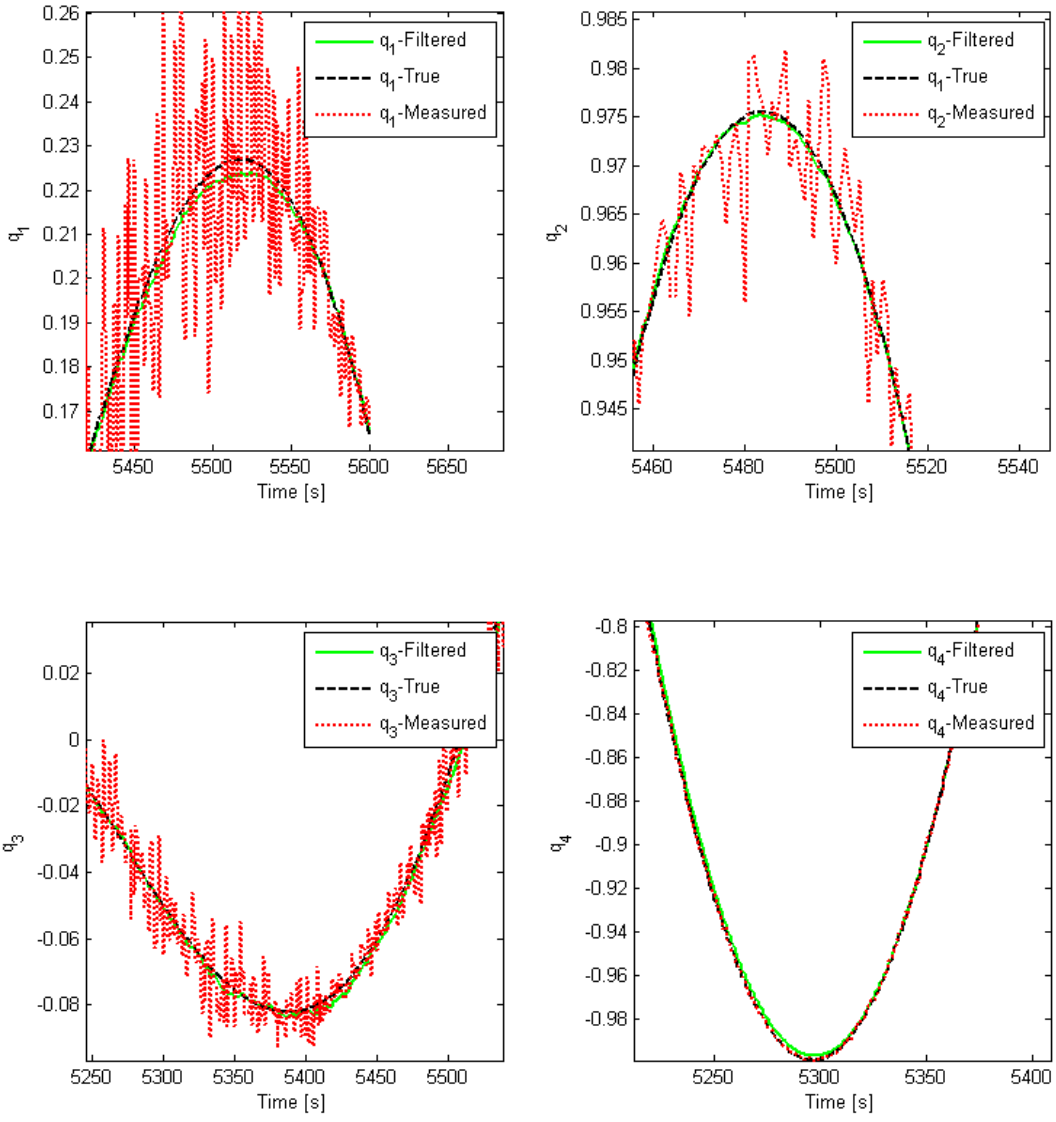

Figure 6.10: Typical Attitude Filter Performance Given Nominal Noise and Tracking Angular Rates

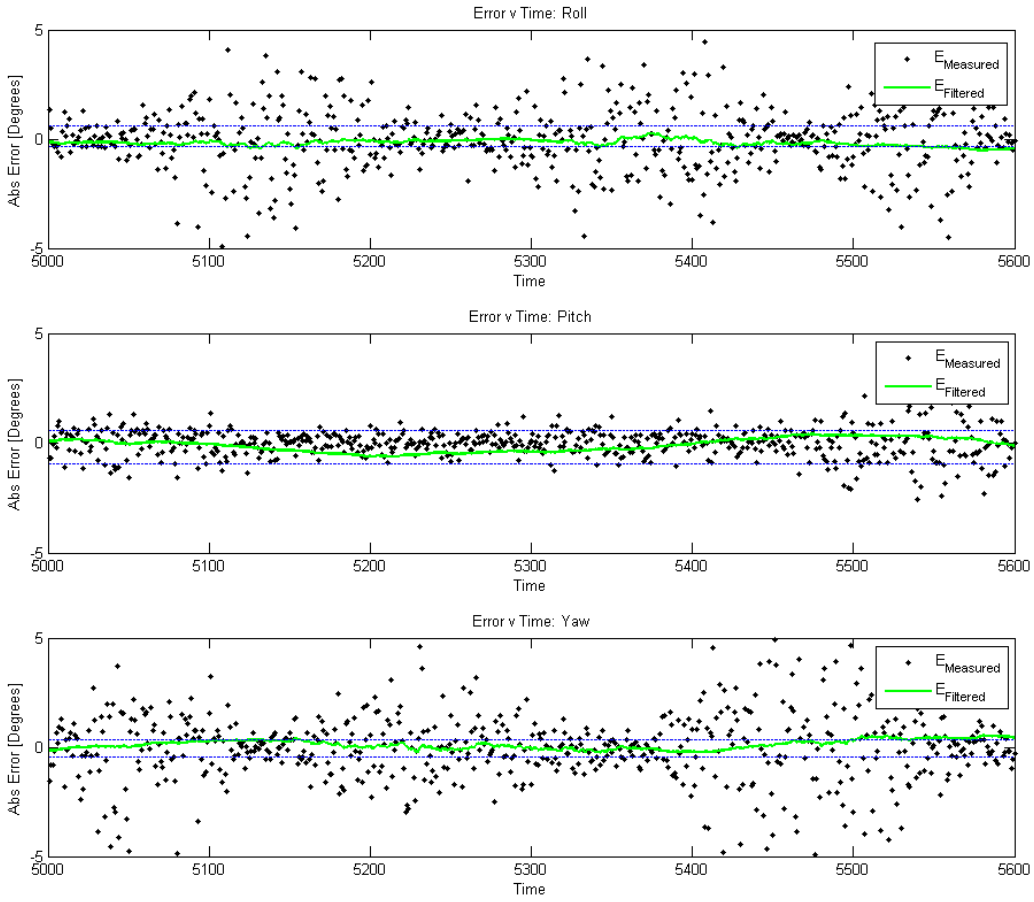

Figure 6.11: Refined Typical Attitude Filter Angular Error Given Nominal Noise and Tracking Angular Rates

CHAPTER 7

RECOMMENDATIONS AND FUTURE WORK

7.1 Recommendations

Several concepts for attitude determination have been explored. In particular, an extended Kalman filter was developed to attain accurate angular rate knowledge, while a standard Kalman filter was developed to attain accurate attitude knowledge. In addition to this, an algorithm was constructed to estimate the angular rates based off of sequential vector measurements.

It is recommended that rate gyros are used to determine the angular rates of the satellite. It has been shown that by using an EKF, the angular rates may be determined to sufficient accuracy in the presence of a large amount of noise. The algorithm to determine angular rates from successive vector measurements may prove useful as a backup or alternative method of determining the spin rate; however, more work needs to be done to improve the method for an axis-symmetric body.

It is also recommended to determine the attitude via the TRIAD algorithm and smooth the results via a Kalman filter. This method provides sufficient accuracy over a wide range of sensor noise levels.

Overall, this system will provide the attitude knowledge and pointing accuracy necessary to support a wide range of scientific missions.

7.2 Future Work

There is a significant amount of work to be done before the attitude determination and control system is flight ready. First, all sensors used must be characterized. It is imparative to understand the noise characteristics of the sensors so that the Kalman filters may be optimized.

Next, the operation of the ADACS must be determined. There are many factors involved in how this software will run on the satellite. This includes the sampling rate of the sensors and the rate and duration of torquing. The configuration of the mission operations that provides for optimal power and time use has yet to be explored.

Last, the software needs to be integrated and tested with the hardware. The ADACS code is currently implemented in MATLAB; it must be compiled for running on the on-board processor. There is much to do to optimize this code for running on this processor. Once this has been completed, full systems tests may

be carried out so that one may be confident in the performance of the system prior to launch.

In addition to making the system ready for flight, an interesting question has been raised by the method for determining angular rates from successive vector measurements. A method for recovering more accurate results with an axis-symetric body has not been achieved. This technique may prove useful for systems with limited sensor, or as an alternative method of rate determination should sensors fail in flight.

Ultimately, much has been accomplished towards completing the attitude determination and control system, yet there is still a significant amount of work to fully implement the system.

REFERENCES

[1] Program, T. C., "CubeSat Design Specification, Rev. 12," Tech. rep., California Polytechnic State University, 2009.

[2] Pukniel, A., *Attitude Determination and Three-Axis Control System for Nanosatellites with Magnetic Torque Actuation*, Master's thesis, University of Illinois at Urbana-Champaign, 2006.

[3] Gregory, B. S., *Attitude Control System Design for ION, The Illinois Observing Nanosatellite*, Master's thesis, University of Illinois at Urbana-Champaign, 2004.

[4] Wertz, J., editor, *Spacecraft Attitude Determination and Control*, Reidel, Dordrech ; Boston :, Dordrecht, Netherlands, 1980.

[5] Psiaki, M. L., Martel, F., and Pal, P. K., "Three-axis Attitude Determination via Kalman Filtering of Magnetometer Data," *Journal of Guidance, Control, and Dynamics*, Vol. 13, No. 3, 1990, pp. 506 – 514.

[6] Shuster, M. and Oh, S., "Three-Axis Attitude Determination From Vector Observations," *Journal of Guidance and Control*, Vol. 4, No. 1, 1981, pp. 70 – 77.

[7] Anderson, T., *The Statistical Analysis of Time Series*, Wiley-Interscience, 1994.

[8] Kalman, R., "New approach to linear filtering and prediction problems," *American Society of Mechanical Engineers – Transactions – Journal of Basic Engineering Series D*, Vol. 82, No. 1, 1960, pp. 35 – 45.

[9] Welch, G. and Bishop, G., "An Introduction to the Kalman Filter," Tech. rep., University of North Carolina at Chapel Hill, 2006.

[10] Simon, D., *Optimal State Estimation*, Wiley-Interscience, 2006.

[11] "Invensense Gyroscope Store," December 2009, *http://www.invensense.com/store/index.html*.

[12] Wertz, J. R. and Larson, W. J., *Space mission analysis and design / edited by James R. Wertz and Wiley J. Larson*, Kluwer Academic, Dordrecht ; Boston :, 1991.

[13] Chobotov, V., *Spacecraft Attitude Dynamics and Control*, Krieger Publishing Company, 1991.